A THESIS

On

Role of Deformations in Cluster Radioactivity using Modified Preformed Cluster Model

Submitted in the partial fulfillment of requirement for the award of the Degree of

Master of Science (PHYSICS)

Submitted by: **Gudveen Sawhney**

Roll No.: 30704003

Under the Guidance of

Dr. Manoj Kumar Sharma

(Assistant Professor**)**

School of Physics and Materials Science

THAPAR UNIVERSITY

PATIALA (PUNJAB)-147 004

JUNE 2009

CERTIFICATE

This is to certify that the report entitled "**Role of deformations in Cluster Radioactivity using modified Preformed Cluster Model**" submitted by **Gudveen Sawhney, Roll No. 30704003**, student of M.Sc. (Physics), Thapar University, Patiala, was carried out by her under my supervision. She has not submitted this material for credit towards any other degree at Thapar University, Patiala or at any other university.

13/7/09

(Dr. Manoj. K. Sharma)
Assistant Professor
School of Physics & Materials Science
Thapar University Patiala

13/7/09

(Dr. O. P. Pandey)
Professor and Head
School of Physics &
Materials Science
Thapar University Patiala

13/7/09

(Dr. R. K. Sharma)
Dean of Academic Affairs
Thapar University
Patiala

Dedicated to:

God who gave me life

And

My Lovable Parents who made it worth living

ACKNOWLEDGEMENT

I would have never succeeded in completing my task without the cooperation, encouragement and help provided to me by various personalities. I express my deep sense of gratitude and respect to my guide **Dr. Manoj K. Sharma, Assistant Professor, School of Physics and Material Science, Thapar University, Patiala,** for his keen interest and valuable guidance, strong motivation and constant encouragement during the course of the work. I thank him from the bottom of my heart for introducing me to Nuclear Physics, for his great patience, constructive criticism and myriad useful suggestions apart from invaluable guidance to me. I am sure that the knowledge gained through my association with my supervisor shall go a long way in helping me to realize my goals in life.

My sincere thanks also goes to Dr. O. P. Pandey, Professor and Head School of Physics and Materials Science, Thapar University, Patiala, for providing all the necessary facilities in the department. I also wish to thank all the faculty and staff of the School of Physics and Material Science for their kind support.

My special thanks to Mrs. Shefali Kanwar, Dr. BirBikram Singh and all the Research Scholars, for their timely help, cooperation and good wishes at various stages of my thesis work. I am also thankful to my all classmates for their help and support at every stage during the thesis work.

Last but not the least; I would like to thank my family, without whom I am nothing, to provide me great opportunities, everlasting support, big encouragement and lots of love.

Date: 15th July, 2009

(MS.GUBVEEN SAWHNEY)

Abstract

The cluster decay of deformed parents is studied using the Preformed Cluster Decay Model (PCM) having deformation and orientation effects included in it. The main strength of the model is that it treats the binary fragmentation on equal footing along with very important information regarding structural features of fragmentation process. This facility is not available in other fission and statistical models. The role of deformations and orientations seems to be extremely essential besides shell structure and Q-value consideration in this rare decay process, giving fragments in between α-particles and fission fragments. It is of great interest to see that in what way the inclusion of deformations and orientations effects of the decaying fragments influence the potential energy surface PES behavior. Because of the apparent variation in the PES of the fragmentation process, the preformation probability P_0 and tunneling penetrability gets modified which influences the decay constant and half life times of clusters accordingly. It may be noted that the scattering potential barrier (position as well as height) gets modified with deformation and orientation effects of outgoing fragments thereby effecting tunneling path and hence the penetrability P.

The work carried out in this thesis seems highly relevant in context of present day developments in low energy nuclear structure physics and could provide handful information for the future experiments in the related area.

CONTENTS

PAGE NO.

Certificate 2

Acknowledgement 4

Abstract 5

Contents 6

List of figures 8

List of Tables 9

Chapter 1: Introduction

1.1 Cluster Radioactivity 2

1.2 Experimental Methods Used and the Results Obtained 12

1.3 Gamow factor Calculations 14

1.4 Theories of Heavy Cluster Decays 22

References 24

Chapter 2: Methodology

2.1 Introduction 29

2.2 The Dynamical Cluster Decay Model 29

2.2.1 Oriented Collisions 34

2.3 Quantum Mechanical Fragmentation Theory 36

2.3.1 The Scattering Potential V(R) 39

2.3.2 The Fragmentation Potential V (η) 39

2.4 The Preformed Cluster-decay Model for ground state 43

Decay Of nucleus

References 49

Chapter 3: Calculations and Discussion 53

Of the Results

Chapter 4: Summary and Conclusion 61

List of figures

Fig.1.1 The natural radioactive decay series emanating from uranium-235 ($^{235}_{92}U$) leading to a stable ^{209}Pb along with α particle emission.

Fig.1.2 The nuclear interaction potential for ^{222}Ra$\rightarrow ^{14}$C + ^{208}Pb, calculated as a sum of Coulomb and proximity potentials.

Fig.2.1 Schematic configurations of two (equal/ unequal) axially symmetric, deformed, oriented nuclei, lying in the same plane and for various θ1 and θ2 values in the range 0^0 to 180^0.

Fig.2.2 The scattering potentials for the ^{34}Si cluster decay of parent nucleus ^{242}Cm, i.e. ^{242}Cm$\rightarrow ^{34}$Si + ^{208}Pb, for ^{34}Si considered as a deformed nucleus.

Fig.3.1 Fragmentation potential for the decay of ^{242}Cm$\rightarrow ^{34}$Si + ^{208}Pb at $R_a = R_t + \Delta R$ (ΔR = -0.3 fm) at ℓ = 0 for the case of spherical compared with quadrupole deformation β_2 alone.

Fig.3.2 Preformation probability P_0 as a function of fragment mass A_2 for the decay of ^{242}Cm$\rightarrow ^{34}$Si + ^{208}Pb at $R_a = R_t + \Delta R$ (ΔR = -0.3 fm) at ℓ =0 for the case of deformed β_2 as well as spherical choice.

Fig.3.3 Penetration probability (P) as a function of fragment mass A_2 for the decay of ^{242}Cm$\rightarrow ^{34}$Si + ^{208}Pb at $R_a = R_t + \Delta R$ (ΔR = -0.3 fm) at ℓ =0 for the case of deformed β_2 as well as spherical choice.

List of Tables

Table 1.1 A summary of the cluster decays studied so far and some of the experimental details.

Table 1.2 Comparison of cluster decay branching ratio, $B_{c} = \lambda_c/\lambda_{\alpha,}$ with the ground state spontaneous fission (SF) data, $B_{SF} = \lambda_{SF}/\lambda_{\alpha,}$ measured in the same experiment, as well as in the earlier experiments where only SF was measured.

Table 3.1 Half-life times and other characteristic quantities for cluster decay of various parent nuclei. The calculations are made by using Preformed Cluster-decay Model (PCM) of Gupta and collaborators, for case of β_2 alone.

Chapter 1

INTRODUCTION

Introduction

Cluster radioactivity is a process in which nucleus emits a fragment that is heavier than an alpha particle but lighter than a fission fragment. The clusters usually emitted in this process are the isotopes of carbon, oxygen, neon, magnesium, silicon etc. When the mass of the cluster fragment becomes comparable with the mass of the daughter, symmetric fission takes place. Thus the cluster radioactivity is an intermediate process between the well known α-decay and the spontaneous fission. In earlier years the cluster radioactivity phenomena was observed mostly in actinide nuclei like radium, uranium etc. Very recently it has been observed that such decays are possible in lower mass region around ^{114}Ba. There has been an exciting experimental detection of the emission of ^{12}C from ^{114}Ba leading to ^{102}Sn, which is attracting a lot of attention and therefore widens the horizon of cluster radioactivity process.

1.1 Cluster Radioactivity

The spontaneous emission of fragments heavier than alpha particle termed as Cluster radioactivity has now become an experimentally confirmed reality. Theoretically, such emissions were first predicted by Sandulescu, Poenaru and Greiner[1]. The first experimental observation was made by Rose and Jones[2]. Encouraged by this, researchers tried to detect other novel modes of radioactive decay in which heavy nuclei disintegrate by emission of intermediate mass fragments. Theoretically, the interest in such decays lies in the estimation of lifetimes, decay constants and branching ratios etc. The lifetimes for the observed cluster fragments of radioactive nuclei have been estimated using various models and compared with the experimental data over last three decades. These models can be classified as the fission models, where only the barrier penetrabilities are calculated, and the preformed cluster models, where the cluster is assumed to be formed before it penetrates the barrier and its preformation probability is also included in the calculations. The physics of the two approaches is apparently different, though it has been possible to look for some similarities between them[3].

To study the phenomenon of cluster radioactivity there are various theoretical models in vogue. The existing models generally fall under two categories: the Unified Fission Model (UFM) and the Preformed Cluster Model (PCM). The physics of the UFM and the PCM are completely different. The UFM considers cluster radioactivity simply as a barrier penetration phenomenon in between the fission and the α-decay without worrying about the cluster being or not being preformed in the parent nucleus. In the PCM clusters are assumed to be preborn in a parent nucleus before they could penetrate the potential barrier with a given Q-value. The basic assumption of the UFM is that heavy clusters as well as the α-particle have equal probability of being preformed where as in PCM, clusters of different sizes have different probabilities of their being preformed in the parent nucleus.

The cluster radioactivity process finds its basis in the fragmentation theory[4-7] where the cold (fusion or fission) reaction valleys are observed[8-11] in the calculated fragmentation potentials. According to these earlier calculations, made for transactinides, cold reaction valleys are generated by the shell closure effects of one or both the reaction partners. For the radioactive nuclei, the role of cold reaction valleys corresponding to the observed cluster-decays was later depicted explicitly by Gupta et al.[12]

Experimentally, the phenomenon of cluster radioactivity as a new basic decay process was established for the first time in the spontaneous ^{14}C decay from ^{223}Ra nuclear system. However, in literature there existed old fission data of Jaffey and Hirsh[13] for ^{24}Ne decay of ^{232}U, which indicates that this phenomenon was already observed as early as 1951, but the authors did not distinguish it from the spontaneous fission process. In a recent experiment, Bonetti et al.[14] have confirmed that the emission of ^{24}Ne from ^{232}U, seen in 1951, could not be due to spontaneous fission (SF) since the then-observed decay constant is larger by an order of magnitude 10^2 than their presently measured upper limiting value of SF decay constant(see Table 1.2 for the parent nucleus ^{232}U) . On the other hand, the old value matches with the measured[14, 15] cluster-decay constants to within only a factor of 5 to 20(see Table 1.1 and 1.2 for decay of ^{232}U). Remember that in any fission two fragments (light and heavy) are

measured simultaneously, in contrast to only one (the light fragment) in exotic cluster decay process.

Following ^{14}C decay from ^{223}Ra many other experiments were placed to strengthen the validity of this concept. Tables 1.1-1.2 summarize the complete experimental information available to date on the new cluster-decay modes of the radioactive nuclei. The complete experimental information on the new cluster-decay modes of the radioactive nuclei is available. As for the multiple branching ratios, so far only three nuclei (^{231}Pa, ^{234}U and ^{238}Pu) are found to decay with the emission of two heavy clusters (other than α particle) but none with more than two. Also, it has now become possible to measure in the same experiment the spontaneous fission probability simultaneously with the cluster decay probability[14] (Table 1.2). The present data indicate that the exotic cluster-decay process is different from the spontaneous fission of radioactive nuclei, since the SF half-lives are, in general, smaller than the cluster decay half-life times. The table 1.1 represents the summary of the cluster decays studied so far along with some experimental observations.

A fine structure, analogous to that observed by Rosenblum[23] in 1929 for α-decay, was also observed[24, 25] for ^{14}C decays of ^{222,223}Ra nuclei. The measurements of cluster decay versus α-decay branching ratios to the excited states of daughter nucleus are observed over the years. This has, so far, been possible only for the ^{14}C branching ratios to the first and second excited states of ^{209}Pb and to the first excited state of ^{208}Pb (see Table 1.1). A few events are also seen corresponding to a transition to the third excited state of ^{209}Pb in ^{14}C decay of ^{223} Ra nucleus. Here again, the calculations of M.Greiner and W.Scheid[26] were made before the experiments.[24] These authors showed that the cluster decay constant can increase by a factor of 5 if decay to excited states of the daughter nucleus are included along with the decay to the ground state. In fact, experiments show that the decay to excited states of daughter nucleus are far more enhanced than to its ground state (Table 1.1).

Table1.1: A summary of the cluster decays studied so far and some of the experimental details.

Decays studied						Experimental cluster decay data		
S.No	Emitted cluster	Parent nucleus	Daughter nucleus	Q value (MeV)	α-decay constant $\lambda(\alpha)s^{-1}$	Branching ratios $B_{expt}(c) = \lambda_c/\lambda_\alpha$	Half lives $T_{1/2}(c)s$	$\log_{10} T^c_{1/2}(s)$
1.	^{14}C	^{221}Fr	^{207}Tl	31.26	$2.40x10^{-3}$	$<4.4 \times 10^{-12}$ $<5.0 \times 10^{-14}$	$>6.5 \times 10^{13}$ $>6.5 \times 10^{15}$	>13.82 >15.80
		^{221}Ra	^{207}Pb	32.39	2.31×10^{-2}	$<4.4 \times 10^{-12}$ $<1.2 \times 10^{-13}$	$>6.8 \times 10^{12}$ $>2.4 \times 10^{14}$	>12.83 >14.38
		^{222}Ra	^{208}Pb	33.05	1.82×10^{-2}	$(3.7\pm0.6) \times 10^{-10}$ $(3.1\pm1.0) \times 10^{-10}$	1.03×10^{11} 1.22×10^{11}	11.01 11.09
		^{223}Ra	^{209}Pb	31.84	7.01×10^{-7}	$(8.5\pm2.5) \times 10^{-10}$ $(7.6\pm3.0) \times 10^{-10}$ $(5.5\pm2.0) \times 10^{-10}$ $(6.1\pm1.0) \times 10^{-10}$ $(4.7\pm1.3) \times 10^{-10}$ $(5.0\pm1.0) \times 10^{-10}$	1.16×10^{15} 1.30×10^{15} 1.80×10^{15} 1.62×10^{15} 2.10×10^{15} 1.98×10^{15}	15.06 15.11 15.25 15.21 15.32 15.30
		^{224}Ra	^{210}Pb	30.53	2.18×10^{-6}	$(4.3\pm1.2) \times 10^{-11}$	7.36×10^{15}	15.87
		^{226}Ra	^{212}Pb	28.21	1.4×10^{-11}	$(3.2\pm1.6) \times 10^{-11}$ $(2.9\pm1.0) \times 10^{-11}$ $(2.3\pm0.8) \times 10^{-11}$	1.57×10^{21} $(1.7\pm0.7) \times 10^{21}$ 2.19×10^{21}	21.20 21.23 21.34
		^{225}Ac	^{211}Bi	30.47	8.02×10^{-7}	$<4.0 \times 10^{-13}$	$>2.5 \times 10^{18}$	>18.40

Continued Table 1.1

S.No	Emitted cluster	Parent nucleus	Daughter nucleus	Q Value (MeV)	α-decay constant $\lambda(\alpha)s^{-1}$	Branching ratios $B_{expt}(c) = \lambda_{c/} \lambda_{\alpha}$	Half lives $T_{1/2}(c)s$	$\log_{10} T^{c}_{1/2}(s)$
		^{226}Th	^{212}Po	30.67	3.74×10^{-4}	$<9.3\times10^{-13}$	$>2.0\times10^{15}$	>15.3
2.	^{18}O	^{226}Th	^{208}Pb	45.88		$<9.3\times10^{-13}$	$>2.0\times10^{15}$	>15.3
	^{20}O	^{228}Th	^{208}Pb	44.72	1.15×10^{-8}	$(8.1\pm3.3)\times10^{-14}$	7.5×10^{20}	20.87
3.	^{23}F	^{231}Pa	^{208}Pb		6.78×10^{-13}	$<2.5\times10^{-13}$ 1.0×10^{-15}	$>4.1\times10^{24}$	>24.61
4.	^{22,24}Ne	^{230}U	^{208,206}Pb	61.59 61.55	3.86×10^{-7}	$<1.1\times10^{-12}$ $<1.1\times10^{-12}$	$>1.6\times10^{18}$ $>1.6\times10^{13}$	>18.2 >18.2
5.	^{24,26}Ne	^{234}U	^{210,208}Pb		9.01×10^{-14}	$(6.6\pm1.3)\times10^{-13}$ $(3.8\pm1.1)\times10^{-13}$	$(1.2\pm0.3)\times10^{25}$ $(1.9\pm0.5)\times10^{25}$	25.06 25.30
		^{235}U	^{211,209}Pb	57.36	3.13×10^{-17}	$<5.0\times10^{-13}$ $<7.8\times10^{-13}$	$>4.40\times10^{28}$ $>2.83\times10^{28}$	>28.64 >28.45

Table 1.2: Comparison of cluster decay branching ratio, $B_c = \lambda_c/\lambda_\alpha$, with the ground state spontaneous fission (SF) data, $B_{SF} = \lambda_{SF}/\lambda_\alpha$, measured in the same experiment, as well as in the earlier experiments where only SF was measured. The SF here means the most probable (symmetric or nearly symmetric) fission fragments.

Both Cluster decay and SF measured simultaneously					Only SF measured	
Parent nucleus	Emitted Cluster	$B_c = \lambda_c/\lambda_\alpha$	$B_{SF} = \lambda_{SF}/\lambda_\alpha$	Ref.	$B_{SF} = \lambda = \lambda_{SF}/\lambda_\alpha$	Ref.
^{232}U	^{24}Ne	$(8.85\pm0.75)\times10^{-12}$	$<1.04 \times 10^{-14}$	14	$(8.94\pm6.21) \times 10^{-13}$	13
	^{28}Mg	$<5.04 \times 10^{-14}$				
^{234}U	^{24}Ne	$(6.61\pm1.30) \times 10^{-13}$	1.29×10^{-11}	19	1.72×10^{-11}	71
	^{28}Mg	$(2.22\pm2.98) \times 10^{-13}$				
^{241}Am	^{34}Si	$<4.2 \times 10^{-13}$	$(2.4\pm0.5) \times 10^{-12}$	70	$(1.9\pm0.7) \times 10^{-12}$	72
		7.4×10^{-16}	7.2×10^{-12}	22	$(3.76\pm0.08) \times 10^{-12}$	73

We observe from Table1.1 and 1.2 a few points that are of special interest:-

1. The half-lives, $T_{1/2}(c)$, are of the order of 10^{11} to 10^{25}s (equivalently, the decay constant $\lambda \sim 10^{-11}$ to 10^{-25} s^{-1}), increasing almost linearly with the size (mass) of the emitted cluster.

2. Many times, only $T_{1/2}(\alpha)/ T_{1/2}(c)$ or $\lambda(c)/ \lambda (\alpha)$, called the branching ratio B, is given, since the α particle always competes with the heavy cluster emission. The experimental values of B are $\sim 10^{-10}$ to 10^{-14}, and do not vary linearly with the size of the emitted cluster because $T_{1/2}(\alpha)$ have values from some seconds to millions of years. Hence, any systematic of the observed data are expected to be given by half life time and not by the Branching ratio.

3. Just as for α decay, the odd parents have $T_{1/2}(c)$ larger than that for the even parents, the so called odd-even parent effect. This effect is $\sim 10^2$ for ^{14}C and ^{24}Ne decays and is to be compared with $\sim 10^1$ for α decay.

4. The decay to ground state is hindered as compared to the excited states for the odd-even parents. This has also been true for α decay as well.

5. All the observed clusters are neutron rich, non α and, except for ^{23}F, even-even nuclei. This means that they are not simply the aggregates of α-particles.

6. ^{34}Si is the heaviest cluster observed so far, which is rather far from the lightest spontaneous fission fragment measured to date. In other words, the limiting value of the mass asymmetry for the cluster decay or the normal fission are not yet established and hence the question remains – where does the cluster decay stop or the normal fission process begin? It is also possible that the two processes overlap for some range of mass asymmetry. Very recently, the attempts were made[27] to observe the very light "cold fission" products (the products with maximum kinetic energy) of the size of the above mentioned exotic clusters. This would open up many new questions and possibilities, some of which are being studied in recent times.

7. The daughter nucleus is always a neutron/proton (or both) closed shell, or nearly closed shell spherical nucleus. This was the starting point based on earlier calculations which led the authors to predict the new cluster radioactivity. In the earlier calculations the minima in the calculated fragmentation potential energy surface always referred to at least one spherical closed shell nucleus. This means that, physically, cluster

radioactivity is not an isolated phenomenon in nature, and must be related to other phenomenon like the cold fusion and cold fission where similar closed shell effects are known to play an important role. This problem was recently discussed in detail by Gupta et al[28]. Furthermore, the question of only the spherical or both the spherical and deformed closed shell effects becomes relevant, since stable deformed closed shell effects were also recently found to exist in nuclei [29, 30]. However no experimental data on cluster radioactivity referring to deformed daughters exists at present.

Theoretically, the question arises whether all the three observed phenomena of α decay, heavy cluster and the spontaneous fission are simply the three cases of a unified fission process with super-asymmetric, asymmetric and nearly-symmetric fission fragments or, alternatively, both α and heavy cluster decays are identical and follow the Gamow theory of α- decay but are different from the spontaneous fission process. Both of these possibilities have been studied[31-66]. In one case[46-60], within the Gamow theory, the α particle as well as the heavy cluster (or clusters) were assumed to be preborn in a parent nucleus before they could penetrate the potential barrier with a given Q-value. Thus, in such a model, called the "Preformed Cluster Model (PCM)", clusters of different sizes have different probabilities of their preformed in the parent nucleus. The barrier assault frequencies are also different for different clusters. In the other case of fission process, two alternative approaches have been followed. In one approach[31-45], Gamow's idea of quantum mechanical barrier penetration is still used, but worrying about the cluster being or not being preformed in the parent nucleus. From this point of view, cluster radioactivity is considered simply as a barrier penetration phenomenon, in between the fission and α-decay. In other words, such a theory, called the "unified fission model (UFM)", does not distinguish between the three processes of α-decay, heavy cluster-decay and fission. In the other fission approach[57-59, 61-66], the parent nucleus is considered to deform continuously and reach the saddle or scission shape.

Apparently, the fission theories are applied to understand the cluster decay process. In the saddle point fission (SPF) model, the mass and charge distributions of all the fragments are assumed to be decided at the saddle point, after the decaying system

has penetrated the barrier. This assumption is based on an earlier calculation where an explicit time –dependant Schrodinger equation, in relative coordinate and the mass and the charge –asymmetry coordinates, was solved. Apparently, here both the barrier penetrabilities and assault frequencies are independent of the fragment (or cluster) sizes, but difficult to calculate. In one of the scission point fission models, the authors consider that the decaying nucleus first arrives at the touching configuration, and then penetrates the barrier.

This model apparently uses the concept of a continuously deforming shape of a fissioning nucleus up to the touching configuration but then uses the interaction barrier of the already separated fragments, since it is only in such potentials (used in UFM) that the touching configuration is known to lie before the barrier height. In another scission point like fission model[65, 66], the neck degree of freedom is also included and, along with the minimization of the action integral, a second order differential equation is solved in a multidimensional deformation space. Then, there are other theories which introduce many new exotic ideas but are not yet studied in detail.

Considering that spontaneous cluster-decay competes with the α particle emission and distinguishes itself completely from normal spontaneous fission, a new definition of radioactive nuclei was suggested namely: a radioactive nucleus was one which decays spontaneously to other stable nuclei not only by fission but also by emitting a cluster (or clusters) heavier than α particle, the α particle itself, the β particle and the γ ray, or any combination of these. The branching occurs more often between α and β decays but also rarely between the α particle and the heavy cluster (or clusters). This definition would be more relevant if use of heavy clusters in radiation studies of biological samples could be established. We illustrate this definition in fig 1.1 for ^{14}C decay of ^{223}Ra, which itself occurs in the natural radioactive series emanating from ^{235}U. Theoretically, many other “by pass” modes are expected to occur. Figure 1.1 clearly shows the decay process of uranium-235 ($^{235}U_{92}$), leading to a stable ^{209}Pb along with α particle emission. Such a decay sequence is important to understand a typical cluster decay process.

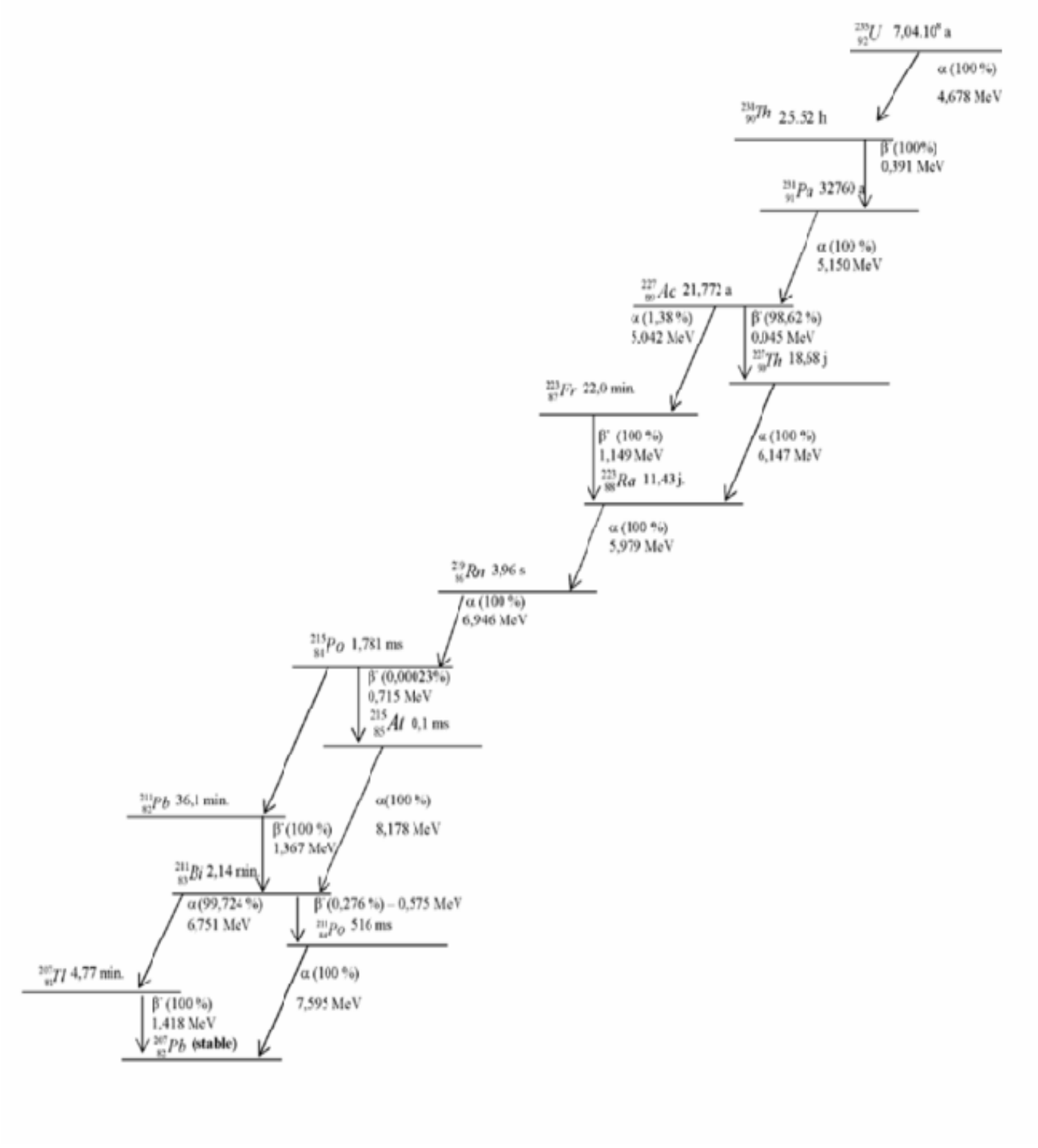

Figure 1.1: The natural radioactive decay series emanating from uranium-235 ($^{235}_{92}U$) leading to a stable ^{209}Pb along with α particle emission.

1.2 Experimental Methods Used and the Results Obtained

Some experimental methods in detecting the spontaneous decay of radioactive nuclei via emission of clusters heavier than α particles were performed. It was found that the observed decay modes are rather rare, and hence exotic. These exotic decay modes were elusive because of the earlier experimental inabilities to distinguish between these rare decay modes and the multiple pile up of α-particle pulses. In the pioneering experiment of Rose and Jones[2], the events due to pile up were rejected by separating the individual α-particles in the events by ~100ns in time. These authors used a solid state (Si) counter telescope that detected α-particles at the rate of ~4000/s in a solid angle of $\frac{1}{3} sr$. The standard ΔE-E method was used. After a run of 189 days, a group of eleven events, with a total energy of ~30 MeV was observed. Although no mass determination was possible in this experiment, on examining the measured Q-value and branching ratio with respect to simple theoretical estimates based on Gamow theory of α-decay, authors[2] concluded that these eleven events were due to the new ^{14}C cluster radioactivity of ^{223}Ra. The source used in this experiment was ^{227}Ac (half –life $T_{1/2}$=21.773y) with which the lower members of the ^{235}U series, including ^{223}Ra, are in secular equilibrium. Using a similar set up and technique, independently, Aleksandrov et al.[17] observed seven carbon events in 30 days. Their work was published a few months later than that of Rose and Jones. The work of Aleksandrov et al. was motivated by the theoretical suggestion of Sandulescu Poenaru and Greiner[1].

This discovery was confirmed by Gales who used the same but more intense (~60 times) source and a magnetic spectrometer (SOLENO) with a large solid angle of $\frac{1}{20} sr$ to $\frac{1}{10} sr$. Thus the collection time for an observation of a group of eleven events at the expected location of ^{14}C beam, was reduced to only 5 days. These authors then repeated their experiment for $^{222,226}Ra$ and ^{241}Am nuclei, and established ^{14}C decays of $^{222,226}Ra$ and set an upper limit for the emission of ^{34} Si decay from ^{241} Am, which is ~10^{-12} for the branching ratio relative to α particle. It was observed that this negative

result of not observing ^{34}Si decay of ^{241}Am still holds well even with the better class of detectors(the glass detectors with upper limits~10^{-16} for branching ratios) used to date. Spontaneous emission of ^{14} C from ^{223} Ra was further confirmed by the use of ^{227}Th source and an Engesplit –pole magnetic spectrograph[18]. This spectrograph permitted an accurate calibration with a "mixed" beam of ^{12}C, ^{13}C and ^{14}C ions, operating in a mode used for detection of long lived radioisotopes. The spectrograph allows mass determination from a measurement of magnetic rigidity and total energy in the focal plane detector. In 6 days of decay counting, twenty four ^{14}C were observed. Thus, we notice how the collection time decreased from some hundred days to only a few days with the improved detection techniques.

Within a year of the work of Rose and Jones, Price et al.[16], in more direct technique using a plastic or glass detectors, reconfirmed this discovery by using the polycarbonate track-recording films and sources of ^{221}Fr and $^{221\text{-}224}$Ra produced by the ISOLDE on-line separator at CERN. All later experiments have used such detectors, since they have the advantage of being insensitive to particles with the ionization rate below that of the particle to be detected. For example, in the experiments of the Price et al.[16], plastic detectors (polycarbonate films) were sensitive to carbon nuclei (Z≥5) but not to α particles. Use of similar plastic track detectors by Barwick et al.[15] with a ^{232}U source resulted for the first time in detecting the emission of ^{24}Ne from ^{232}U. In later experiments that resulted in the discovery of ^{20}O, ^{23}F, ^{28,30}Mg and ^{32,34}Si decays (in addition to other ^{24,26}Ne decays), the plastic detectors were replaced by the phosphate glass detectors because of their better discrimination against α-particles.

The fine structure of ^{14}C radioactivity from ^{222,223}Ra is observed by using an intense source and better energy resolution. In both cases the magnetic Spectrometer SOLENO was used to focus the emitted ^{14}C ions on a single Si detector. A single Si detector, rather than a telescope, was enough, since the nature of decay was already established in the previous experiments. This resulted in a high quality energy spectrum. These experiments established that cluster radioactivity and α-decay are similar processes.

Finally, in Table 1.2 we find that spontaneous fission (most probable symmetric or nearly-symmetric fission fragment) of some nuclei is also measured along with the

heavy cluster decay. The spontaneous fission rates are, in general, an order of magnitude higher then the cluster decay rates. It is rather straightforward to measure both of these processes since the range of fission fragments in only about the half of the range of the nuclei so far observed in cluster radioactive decays[19, 22]. The phosphate glass detectors are ideally suited for detection of both the heavy clusters and the spontaneous fission tracks. Also, the shape of fission tracks is different from the cluster tracks, which are themselves different for different clusters. Apparently, many more simultaneously measurements of spontaneous fission and heavy cluster-decays are in the offing. This should further establish that cluster radioactivity is more of an α decay like rather than the fission like process. As mentioned earlier, for every heavy cluster emissions, the two processes are likely to overlap and make contributions to the decay half lives etc.

1.3 Gamow Factor Calculations (Coulomb-plus-Square-Well Potential)

We are dealing here with a phenomenon where the theory has superseded the experiments. This happens rather rarely, and in this case, the theoretical calculations of Sandulescu, Poenaru and Greiner[1] predicted this new phenomenon of cluster radioactivity before it was observed experimentally by Rose and Jones[2]. Sandulescu et al. used two limiting approaches of

1. The super-asymmetric fission as a dynamical mass fragmentation[4-11], and

2. The strongly asymmetric two body fragmentation as emission of heavy clusters through a barrier, like in Gamow theory of α decay.

Thus, a new decay mode, intermediate between fission and α decay, was predicted. In the following we first discuss the very simple minded Gamow factor calculations made for heavy cluster emissions in an almost original form of using the Coulomb-plus-square-well potential, like for α-decay. These calculations have been of great interest for studying the systematic variations of the measured quantities.

The basic assumptions of Gamow's theory are:

1. An α particle may exist as an entity within a heavy nucleus.

2. Such a particle is in constant motion and is contained in the nucleus by the surrounding potential barrier.

3. There is small but definite –likelihood that the particle may pass through the barrier (despite its height) each time a collision with it occurs.

Alpha particle decay arises as a consequence of quantum-mechanical tunneling through a potential barrier; that is, the alpha particle penetrates the potential barrier instead of going over the top as demanded by classical physics. The calculation assumes that the alpha particle is pre-formed in the nucleus before being emitted in the decay process. Once it has been emitted, the alpha particle gains its final kinetic energy by electrostatic repulsion as it moves away from the residual nucleus.

Gamow theory of α decay[67] is based on the concept of a preformed α Particle tunneling through essentially a Coulombic barrier due to the α particle and the daughter nucleus. Considering a one dimensional WKB penetration problem through a coulomb-plus-square-well-potential of width $R = r_0(A_1^{1/3} + A_2^{1/3})$, the decay constant λ_G defined as:

$$\lambda_G = \nu_0 P\,, \tag{1.1}$$

where ν_0 is the escape frequency with which the alpha particles bombard the walls of the barrier. One can also call ν_0 as the frequency of existence of α particles at the barrier. For an α particle with energy Q, the WKB penetration probability P through a coulomb potential (see Fig 1.2, solid line) is

$$P = \exp(-2G)\,, \tag{1.2}$$

with G, the Gamow factor, given as

$$G = \frac{1}{\hbar}\int_{R_a}^{R_b}\left(2\mu\{E_c(r)-Q\}\right)^{1/2}\,dr \tag{1.3}$$

Here, $E_c(r) = \frac{Z_1 Z_2 e^2}{r}$ is the coulomb potential, $\mu = m\frac{A_1 A_2}{A}$ is the reduced mass of the system with m as nucleon mass, and R and R_b are, respectively the inner and outer turning points. $R_b = \frac{Z_1 Z_2 e^2}{Q}$, the value of r where $E_c(r) = Q$, the Q-value of the reaction or, in the present case, the α particle decay energy. The subscripts 1 and 2 refer to α particle and the daughter nucleus, respectively. The integral in Eq. (1.3) has an analytical solution, giving

$$G = \frac{1}{\hbar}\sqrt{\frac{2\mu}{Q}}Z_1 Z_2 e^2\left(\arccos\sqrt{x} - \sqrt{x(x-1)}\right), \tag{1.4a}$$

with
$$x = \frac{R}{R_b} = \frac{r_0\left(A_1^{1/3} + A_2^{1/3}\right)Q}{Z_1 Z_2 e^2} = \frac{Q}{V_B} \tag{1.4b}$$

Here,
$$V_B = \frac{Z_1 Z_2 e^2}{R} \tag{1.4c}$$

is the coulomb barrier height. In Eq. (1.4) all quantities are known, except r_0 which is traditionally taken as a parameter to be fitted to the experimental data. Also, different authors have used different values of α particle preformation factor ν_0 in Eq. (1.1).

The following figure 1.2 shows the schematic potential energy surface V(R) for α particle decay of the nucleus. The solid line shows the idealized Coulomb plus square well potential, used in Gamow theory for α decay. The dashed line shows the rounding of the potential due to the nuclear effects.

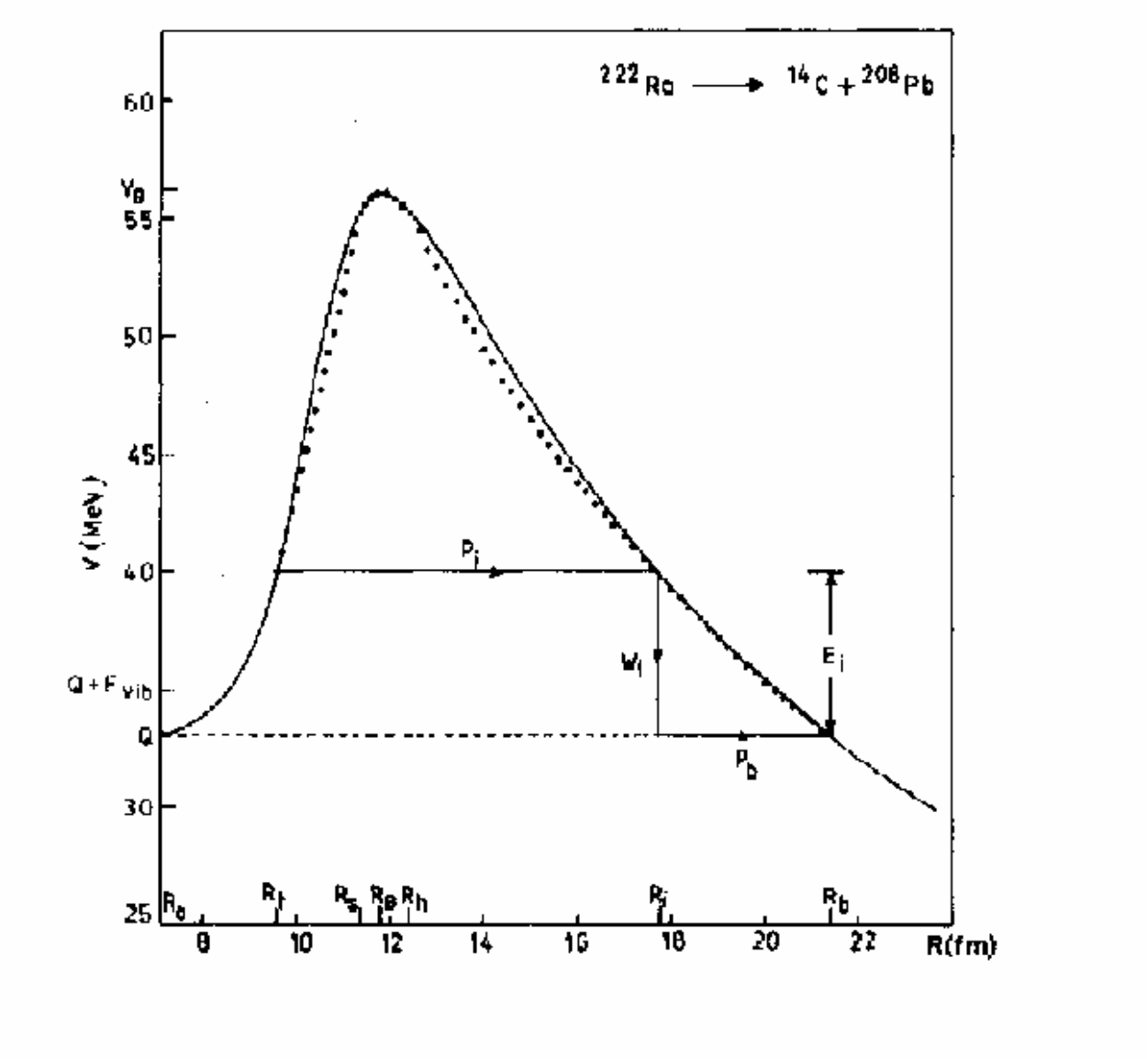

Figure 1.2: The nuclear interaction potential for $^{222}Ra \rightarrow ^{14}C + ^{208}Pb$, calculated as a sum of Coulomb and proximity potentials (solid lines). The path of tunneling is also shown, the dotted lines show the parameterized potential used to calculate the penetrability analytically.

The nature of the function in Eq. (1.4) is rather simple and becomes evident if we make a Taylor expansion about x=0. We obtain

$$\ln P = \frac{\sqrt{2\mu V_B}}{\hbar} R\left(\frac{\pi V_B^{1/2}}{Q^{1/2}} - 4 + \frac{Q}{V_B} - \frac{3V_B^2}{4Q^2} + ... \right) \tag{1.5}$$

This relation shows that $\ln P$ varies almost linearly with $Q^{-1/2}$, which is taken as a plausibility argument for the straight line description of Geiger –Nuttall plots between $\log_{10} T_{1/2}(s)$ and $Q^{-1/2}$ for each Z:

$$\log_{10} T_{1/2}(s) = aQ^{-1/2}(Mev) + b \tag{1.6}$$

with a and b as constants for each element. The half- life times $T_{1/2}$ are related to decay constant λ as:

$$\lambda = \frac{\ln 2}{T_{1/2}} \tag{1.7a}$$

One can also talk of the decay width,

$$\Gamma = \hbar\lambda \tag{1.7b}$$

Relation (1.6) was tested again very recently by Buck et al., [68, 69] who obtained different values of constants a and b for different α - emitting even-even nuclei with N<126 and N>126. Instead of using the single coulomb condition (1.4c) , these authors have related R and V_B to a global quantum number g (an additional free parameter, not related to G of Eq.(1.2)) through the Bohr- Sommerfield condition for the (preformed) α particle considered in the orbit of the remaining core of the parent nucleus. The calculations are also extended empirically to exotic cluster decays of even-even nuclei by taking both the parameters G and V_B, arbitrarily, proportional to mass number of the emitted cluster.

The barrier penetration theory of α decay is found to be good only for the ground state to ground state transitions in even- even nuclei. Other transitions are observed to be

slower than predicted by the theory and are said to be hindered. This odd-even effect of parent nuclei is denoted by a quantity, called hindrance factor F, which is simply a ratio between the Gamow and measured decay constants:

$$F = \frac{\lambda_G}{\lambda_{\exp t}} = \frac{T_{1/2}^{\exp t}}{T_{1/2}^{G}} \quad , \tag{1.8a}$$

Or, more generally, for any potential

$$F = \frac{\lambda_{cal}}{\lambda_{\exp t}} = \frac{T_{1/2}^{\exp t}}{T_{1/2}^{cal}} \tag{1.8b}$$

with $F = 1$, defined customarily, for all even-even ground state transitions. Such normalization has the advantage of referring the hindrance factors to the ground state rather than to the absolute calculated values.

Rose and Jones[2] used the Gamow theory of α decay for analyzing their pioneering experiment on ^{14}C decay of ^{223}Ra. They calculated the ratios $\frac{\lambda_G(c)}{\lambda_G(\alpha)}$, of Gamow factors, for some likely cluster-decays with respect to α-decay. Using three different values of r_0=1.15, 1.20 and 1.25 fm, they found that ^{14}C decay of ^{223}Ra virtually selects as the most probable one, since the ratio of Gamow factors is the largest. One could have reasonably well expected the preformation probability for ^{12}C to be considerably higher than for the neighboring nuclei, since sequences of three α particles occur in the radioactive decay chain of ^{235}U (figure1.1) with which, as stated before, ^{223}Ra is in secular equilibrium. For this purpose, these authors made an experimental estimate of the preformation probability P_0 by comparing their measured branching ratio $B_{expt}(c)$ ($=\frac{\lambda_{\exp t}(c)}{\lambda_{\exp t}(\alpha)}$, the ratio of measured cluster decay constant) with the calculated ratios of Gamow factors, $\frac{\lambda_G(c)}{\lambda_G(\alpha)}$ ($=B_G(c)$), for various carbon nuclei from ^{223}Ra. They found:

$$\frac{P_0(c)}{P_o(\alpha)} = \frac{B_{\exp t}(c)}{B_G(c)} = \frac{\lambda_{\exp t}(c) \big/ \lambda_G(c)}{\lambda_{\exp t}(\alpha) \big/ \lambda_G(\alpha)} \tag{1.9a}$$

~0.1-10 for ^{12}C, ^{13}C and ^{15}C (1.9b)

= 7x10^{-5}- 4 x10^{-7} for ^{14}C (1.9c)

In view of the rare nature of the heavy cluster decays with respect to α particles these authors termed the numbers in Eq. (1.9b) absurd and unacceptable. Thus, ^{14}C decay of ^{223}Ra was identified and an empirical estimate of its preformation probability with respect to α particle was given by Eq. (1.9c) for the first time.

According to the α decay theory, $P_0(\alpha) = 1$. Therefore, one can take Eq. (1.9c) as a measure of the preformation probability of ^{14}C in ^{223}Ra. Such a point of view has later prompted great interest in the study of empirical trends of P_0, by defining this quantity from (1.9a) for any cluster c, as

$$P_0(c) = \frac{\lambda_{\exp t}(c)}{\lambda_G} \tag{1.10a}$$

Or, more generally, for any other shape of the nuclear potential

$$P_0(c) = \frac{\lambda_{\exp t}(c)}{\lambda_{cal}(c)} \tag{1.10b}$$

In contrast to the above approach of estimating P_0 from Eq. (1.10a), many experiments are analyzed by empirically fitting the Gamow factors to the measured data by measuring either r_0 alone or both r_0 and ν_0 in Eqs. (1.1)-(1.4). This means taking $P_0(c) = 1$ and its effects considered to be assimilated in the varied parameter or parameters. For the best fit to the data, different authors have obtained different values of r_0 or both r_0 and ν_0.

The concept of different r_0 for different clusters is also used by Iriondo et al., [60] who define the formation amplitude of a cluster with respect to the α particle simply as the ratio of the Gamow penetrabilities at r_0 =0.98 and 1.20 fm. The interesting result of this calculation is that the relative formation amplitude are much smaller than one (~10^{-5} to 10^{-17} for ^{8}Be to ^{46}Ar) and decrease with the increasing size of the cluster.

Alternatively, some authors [20, 21] have plotted the measured $\log_{10} T_{1/2}^{\exp t}(s)$ as a function of the calculated $\ln P$ for all ground state transitions of α and heavy cluster decays. It was noticed that for each emitted cluster, the data for even-even parents lie on a straight line. Also, all the straight lines have nearly the same slope. Thus, the heavy cluster decay systematics are similar to that of for α decay. Remember, however, that for α decay the straight lines between $\log_{10} T_{1/2}(s)$ and $Q^{-1/2}$ are for each element, and here it is for each cluster. This result can be considered to mean that the two processes (α decay and heavy cluster decay) are perhaps analogous, but the somewhat different slopes and the different intercepts of these straight lines for different clusters raise the question of associating, say, the different preformation factors P_0 to different cluster decays. This becomes evident if we modify the definition (1.1) of Gamow α decay constant for the cluster decays, to include the preformation factor, as follows:

$$\lambda(c) = \nu_0 P P_0 \qquad (1.11)$$

Notice that here ν_0 is practically a constant ~10^{21}s^{-1} and, as Rose and Jones have shown, it is only through P_0 that λ_G (or equivalently, the $T_{1/2}^{G}$) becomes comparable with $\lambda_{\exp t}$ (or $T_{1/2}^{\exp t}$). A use of more realistic nuclear potential, than simply the square well, would apparently modify the relative magnitudes of P and P_0 but not the above conclusions.

It is relevant to mention here that the Gamow theory of coulomb barrier penetration has been quite successful for giving many systematic of the heavy cluster decays. Interesting enough, the heavy cluster decay is found to behave very much the same as

the α decay. However, a result like that of Eq. (1.11) suggests that the use of a more realistic nuclear potential and the introduction of the concept of different preformation probabilities for different sizes of the clusters are a must in order to make the α decay theory a complete theory for heavy cluster decays.

1.4 Theories of Heavy Cluster-Decays

Most of the theoretical efforts for interpreting the observed heavy cluster-decays have gone towards improving the Gamow's theory of α decay. There are two possible ways that have been followed. In one case, instead of the square well, a more realistic nuclear potential is used. This includes the phenomenological work of analytical super-asymmetric fission model (ASAFM) using a second order polynomial[31-34], a sum of cubic and quadratic parabolas[35], the proximity potential[36,37], the Yukawa plus-exponential potential[38-40], the Cosh potential [41-43](or, equivalently, the double folded potential using Dirac δ- function for two body interaction), and the double folded Michigan -3 Yukawa (M3Y) potential[44,45] etc. Apparently, some of these potentials are derived from the microscopic two body effective interactions and use the cluster and core (daughter nucleus) densities. However, none of these calculations include theoretically the cluster preformation probability P_0 in their works.

It is relevant to collect here that, in view of the rare nature of these heavy cluster decays, Rose and Jones had termed P_0 ~1 or even 0.1 as absurd and unacceptable. We refer to these models with $P_0 \approx$ 0.1-1 as the "unified fission model (UFM)", since some of these[40-45] are essentially the fission models and others could be used to describe all the three processes of α decay, heavy cluster-decays and the spontaneous fission simply by varying the parameters of the nuclear potential used. This is the approach that was used by Sandulescu et al.[1] for obtaining some half- life time estimates in their pioneering work based on the dynamical fragmentation theory.

The other approach for making the α decay theory adaptable to heavy cluster decays is to not only use a more realistic potential, but also to associate with it a cluster

preformation probability P_0 that depends on the size of the emitted cluster. In other words, here the clusters are considered to be preformed in the parent nucleus before they can penetrate the potential barrier. Thus, the nuclear structure information also goes into the development of such a formulism. Both the shell model and collective model bases are used[46-59] for this purpose. We refer to such models as "preformed cluster models (PCM)". Apparently, these models treat the α and heavy cluster decays alike, but differently from spontaneous fission.

Some models have been developed for studying the heavy cluster decay explicitly as a spontaneous fission process. One of these models is "saddle point fission (SPF)" model[61-64] .This model is used for studying the (cold) super-asymmetric fission process, which is shown to compete with the exotic cluster-decay process. The other fission models used for studying the cluster decay as a super-asymmetric fission process are given in Refs. 58, 65 and 66.

In the present work we have used the Preformed Cluster Model (PCM). The details of the model are given in chapter 2.

References

1. A .Sandulescu, D.N. Poenaru and W. Greiner, Sovt. J. Part.Nucl.11, 528(1980).
2. H J Rose amd G A Jones, Nature (London) 307, 245 (1984).
3. D N Poenaru, D Schnabel, W Greiner, D Mazilu and R Gherghescu, Atomic Dat Nucl. Tables 48, 231 (1991).
4. H.J. Fink, W. Greiner, R.K. Gupta et al, Vol.2, p.21.
5. R. K Gupta, Sovt. J. Part. Nucl.8, 289(1977); Nucl. Phys. And Solid St. Phys. (India) A 21, 171(1978).
6. J.A. Maruhn, W. Greiner and W. Scheid, Heavy Ion Collisions, ed. R. Bock (North-Holland, Amsterdam, 1980), Vol. II, Ch.6.
7. R. K.Gupta, D. R. Saroha and N. Malhotra, J. Physique (Paris) Coll. 45, C6-477(1984).
8. A. Sandulescu, R. K. Gupta, W. Scheid and W. Greiner, Phys. Lett. B60, 225(1976).
9. R.K.Gupta, A.Sandulescu and W.Greiner, Phys.Lett.B67, 257(1977); Z.Naturforsch. 32a, 704(1977).
10. R.K.Gupta, C.Parvulescu, A. Sandulescu and W. Greiner, Z. Phys. A283, 217(1977).
11. A. Sandulescu, H. J. Lustig, J. Hahn and W. Greiner, J. Phys. G: Nucl. Phys.4, L279 (1976).
12. R. K. Gupta, S.Gulati, S.S.Malik and R. Sultana, J.Phys. G: Nucl. Phys. 13, L27 (1987).
13. A.H. Jaffey and A.Hirsch, unpublished data, quoted in: R.Vandenbosch and J.R. Huizenga, Nuclear Fission, (Academic Press, New York, 1973)
14. R.Bonetti, E.Fioretto, C.Migliorino, A.Pasinetti, F.Barranco, E.Vigezzi and R.A.Broglia, Phys.Lett.B241, 179(1990).
15. S.W.Barwick, P.B. Price and J.D. Stevenson, Phys.Rev.C31, 1984(1985).
16. P.B.Price, J.D.Stevenson, S.W.Barwick and H.L.Ravn, Phys.Rev.Lett.54, 297(1985).
17. D.V.Aleksandrov, A.F.Belyatskii, Yu.A.Glukhov, E.Yu.Nikol'skii, B.G.Novatskii, A.A.Ogloblin and D.N.Stepanov, JETP Lett.40, 909(1984).

18. W.Kutschera, I.Ahmed, S.G.Armatto III, A.M. Friedman, J.E.Gindler, W.Henning, M.Paul and K.E.Rehm, Phys.Rev.C32, 2036(1985).
19. S.Wang, P.B. Price, S.W. Barwick. K.J.Moody and E.K.Hulet, Phys.Rev.C36, 2717(1987).
20. S.P.Tretyakova, Yu.S.Zamyatnin, N.N.Kovanstev, Yu.S.Korotkin, V.L.Mikheev and G.A.Timofeev, Z.Phys.A333, 349(1989).
21. A.A.Ogloblin, N.I.Venikov, S.K.Lisin, V.M.Shubko, S.P.Tretyakova and V.L.Mikheev, Phys.Lett.B235, 35(1990).
22. K.J.Moody, E.K.Hulet, S.Wang, P.B.Price and S.W.Barwick, Phys.Rev.C36, 2710(1987).
23. S. Rosenblum, C.R. Acad. Sci. Paris 188, 1401 (1929).
24. L.Brillard, A.G. Elayi, E. Hourani, C.R. Acad. Sci. Paris Ser. II309, 1105 (1989).
25. M. Hussonnois, J.F. Ledu, L.Brillard, J. Dalmasso and G. Ardisson, Phs. Rev. C43, 2599(1991).
26. M. Greiner and W. Scheid, J. Phys. G: Nucl. Phys. 12, L229 (1986).
27. (a)B.Borsig, F.Gonnenwein, U.Graf, H.Faust; (b)F.Gonnenwein, Proc.NATO Advanced Study Institute, Frontier Topics in Nuclear Physics, Predeal, Romania, Aug. 24-Sep.4, 1993, eds. W.Scheid and A.Sandulescu(Plenum), to be published.
28. R. K. Gupta, S. Singh, W. Scheid and W. Greiner, J.Phys. G: Nucl. Part. Phys. 18, 1243(1992).
29. R.K. Gupta, W. Scheid and W. Greiner, J.Phys. G: Nucl. Part. Phys. 17, 1731(1991).
30. R. K Gupta, S. Singh, R.K. Puri and W. Scheid, Phys. Rev. C47, 561(1993).
31. D.N.Poenaru, W.Greiner, M. Ivascu and A.Sandulescu, Phys. Rev. C32, 572(1985); J.Phys.G:Nucl.Phys.10, L183 (1984).
32. D. N. Poenaru, W. Greiner, K. Depta, At. Data Nucl. Data Tables 34,423(1986).
33. D. N. Poenaru, D.Schnabel, W.Greiner, D.Mazilu and R.Gherghescu, At. Data Nucl. Data Tables 48,231(1991).

34. D.N.Poenaru, W.Greiner, M. Ivascu and A.Sandulescu,Phys. Rev.C32, 2198(1985); D.N.Poenaru, W.Greiner and R.Gherghescu, Phys.Rev.C47, 2030 (1993).
35. G. A. Pik-Pichak, Sovt. J. Nucl. Phys.44, 923(1986).
36. (a)Y. J. Shi and W.J. Swiatecki, Nucl. Phys. Rev. Lett54, 300(1985); (b) Y.J.Shi and W.J.Swiatecki, Nucl.Phys.A438, 450(1985).
37. Y. J. Shi and W.J. Swiatecki, Nucl. Phys.A464, 205(1987).
38. G. Shanmugam and B. Kamalaharan, Phys, Rev. C38, 1377(1988).
39. G. Shanmugam and B. Kamalaharan, Phys, Rev. C41, 1184(1990).
40. G. Shanmugam and B. Kamalaharan, Phys, Rev. C41, 1742(1990).
41. B. Buck and A.C. Merchant, J. Phys. G: Nucl. Part.Phys. 15, 615(1989); (b) B.Buck and A.C.Merchant, Phys.Rev.C39, 2097(1989).
42. B. Buck and A.C. Merchant and S.M.Perez, Nucl. Phys. A512, 483(1990)
43. B. Buck and A.C. Merchant, J. Phys. G: Nucl. Part.Phys. 16, L85(1990)
44. A. Sandulescu, R.K. Gupta, F. Carstoiu, Int. J. Mod. Phys. E1, 379(1992).
45. R.K. Gupta, A. Sandulescu and M. Greiner and W.Scheid, J. Phys. G: Nucl. Part.Phys. 19, 2063(1993).
46. R.Blendowske, T.Fliessbach and H.Walliser, Nucl.Phys.A464, 75(1987).
47. R.Blendowske, T.Fliessbach and H.Walliser, Z.Phys.A339, 121(1991).
48. R.Blendowske, T.Fliessbach and H.Walliser, Preprint prepared for handbook of Nuclear Decay Modes 1992, ed.D.Poenaru.
49. R.Blendowske and H.Walliser, Phys.Rev.Lett.61, 1930(1988).
50. M. Ivascu and I. Silisteanu, Nucl. Phys.A485, 93(1988).
51. S. G. kadmensky, W. I. Furman and Yu. M. Chuvilskii, Sovt. J. Izv. Akad. Nauk. SSSR, ser. Fiz. 50, 1786(1986).
52. R. K. Gupta, Invited Review Talk at Seventh National Symposium on radiation Physics, Mangalore, india, Nov. 16-20, 1987.
53. R. K. Gupta, Proc. Vth Int. Conf. on Nucl. Reaction Mechanisms, Varenna, Italy, 1988, p.416.

54. S. S. Malik and R. K. Gupta, Phys. Rev. C39, 1992(1989).
55. R.K. Gupta, IANCAS Bull. (India) 6, 2(1990).
56. V. A. Rubchenya, V.P. Eysmont and S.G. Yavshits, Izv. Akad. Nauk. SSSR, ser. Fiz 50, 1017(1986).
57. F.Barranco, R.A.Broglia and G.F.Bertsch, Phys.Rev.lett.60, 507(1988).
58. F.Barranco, R.A.Broglia and E.Vigezzi, Phys.Rev.C39,2101(1989).
59. F.Barranco, R.A.Broglia, E.Vigezzi and G.F.Bertsch, Nucl. Phys.A512, 253(1990).
60. M.Iriondo, D.Jerrestam and R.J.Liotta, Nucl.Phys.A454, 252(1986).
61. S. Kumar, S. S Malik and R. K Gupta, Nucl. Phys. Symp. (India) B31, 61(1988).
62. R.K.Gupta, S.Kumar, H.Kumar, W.Scheid and W.Greiner, 7th Adriatic Int.Conf. On Nucl.Phys., Brioni, Yugoslavia, May 27-June1, 1991, p.5.
63. S. Singh, Ph.D. Thesis 1992, Panjab University, Chandigarh, India (unpublished).
64. S. Kumar, R.K.Gupta and W.Scheid, Int.J.Mod.Phys.E3, No.1(1994)
65. (a) W.Greiner and A.Sandulescu, J.Phys.G:Nucl.Part.Phys.17, S429(1991);
    (b) K.Depta, W.Greiner, J.A.Maruhn, H.J.Wang, A.Sandulescu and R.Herman, Frankfurt Preprint 1992.
66. D.N.Poenaru, M.Mirea, W.Greiner, I.Cata and Z.Mazilu, Mod. Phys .Lett. A5, 2101(1990).
67. I.Perlman and J.O.Rasmussen, “Alpha radioactivity” in Handbuch der Physik, Vol.XLII, ed.S.Flugge, (Springer Berlin, 1957), p.109.
68. B.Buck, A.C.Merchant and S.M.Perez, Phys.Rev.Lett.65, 2975(1990); J.Phys.G:Nucl.Part.Phys.17, 1223(1991).
69. B.Buck, A.C.Merchant and S.M.Perez, J.Phys.G:Nucl.Part.Phys.17, L91(1991); J.Phys.G:Nucl.Part.Phys.18, 143(1992).
70. M.Paul, I.Ahmad and W.Kutschera, Phys.Rev.C34, 1980(1986).
71. H.R.von Gunten, A.Grutter, H.W.Reist and M.Baggentos, Phys.Rev.C23, 1110(1981).
72. V.A.Druin, V.L.Mikheev and N.K,Skobelev, Sovt.Phys.JETP 13, 889(1961).
73. R.Gold, R.J.Armani and J.H.Roberts, Phys.Rev.C1, 738(1970).

Chapter 2

METHODOLOGY

2.1 Introduction

In the present work, we plan to use the dynamical model (DCM) which is based on the well established quantum mechanical fragmentation theory (QMFT). The main advantage of DCM over the statistical models is that it treats the LP's (with fragment mass $A_2 \leq 4$) and IMF's (cluster heavier than α-particles and lighter than symmetric and near symmetric fission fragments) on equal footings, whereas in all other statistical models the LP's and IMF's are treated differently. Another important feature of DCM is that it involves the preformation probability P_0 of the fragments and hence imparts the important information regarding structure of decaying nuclear system.

2.2 The Dynamical Cluster- decay Model

The dynamical cluster-decay model[1] is an adaptation of the preformed cluster model (PCM) of Gupta et al[2,3] for ground state decays, which itself is based on the well-known Quantum Mechanical Fragmentation Theory, the QMFT[4-6,] given for fission and heavy ion reactions. This theory is worked out in terms of the collective coordinates of mass asymmetry $\eta = (A_1 - A_2)/(A_1 + A_2)$ and relative separation R, which in a PCM allows defining the decay half-life $T_{1/2}$, or the decay constant λ, as

$$\lambda = \frac{\ln 2}{T_{1/2}} = P_0 \nu_0 P \qquad (2.1)$$

where the preformation probability P_0 refers to η motion and the penetrability P to R motion. Apparently, the two motions are taken as decoupled, an assumption justified in the earlier works[4, 5, 7]. The ν_0 is the barrier assault frequency. In terms of the partial waves, the decay cross-section

$$\sigma = \frac{\pi}{k^2}\sum_{l=0}^{l_c}(2l+1)P_0P \ ; \qquad k = \sqrt{\frac{2\mu E_{c.m}}{\hbar^2}} \tag{2.2}$$

with $\mu = [A_1A_2/(A_1+A_2)]\,m = \frac{1}{4}Am\ (1-\eta^2)$ the reduced mass, l_c (the critical angular momentum), and m is the nucleon mass. This means that λ in Eq. (2.1) gives the s-wave cross-section, with a normalization constant ν_0, instead of the π/k^2 in Eq. (2.2). For η-motion, we solve the stationary Schrödinger equation in η, at a fixed R,

$$\left\{-\frac{\hbar^2}{2\sqrt{B_{\eta\eta}}}\frac{\partial}{\partial\eta}\frac{1}{\sqrt{B_{\eta\eta}}}\frac{\partial}{\partial\eta}+V_R(\eta,T)\right\}\psi^{\nu}(\eta) = E^{\nu}\psi^{\nu}(\eta) \tag{2.3}$$

with ν=0,1,2,3,.....and $R = R_a = C_t\,(=C_1+C_2)$, the first turning point, fixed empirically for the ground state $(T=0)$ decay. This value of R (instead of the compound nucleus radius R_0) assimilates to a good extent the effects of both deformations β_i of two fragments and neck formation between them[8]. The deformation effects of nuclei in the calculations are further included via the Suessmann central radii $C_t = R_i - (b^2/R_i)$, with radii $R_i = 1.28A_i^{1/3} - 0.76 + 0.8A_i^{-1/3}$ fm and the surface thickness parameter $b = 0.99$ fm.

The Eigen solutions of Eq. (2.3) give the preformation probability

$$P_0 = \sqrt{B_{\eta\eta}}\left|\psi[\eta(A_i)]\right|^2(2/A), \tag{2.4}$$

(i=1 or 2), where $\psi(\eta)$ is $\psi^{\nu=0}(\eta)$ if the ground-state solution is chosen.

However, for the decay of a hot compound nucleus, we use an ansatz[7] for the first turning point,

$$R_a = C_t(\eta,T) + \Delta R(\eta,T), \tag{2.5}$$

which depends on the total kinetic energy TKE(T). The corresponding potential $V(R_a)$ acts like an effective, positive Q value, Q_{eff} for the decay of the hot compound nucleus at temperature T to two fragments in the exit channel observed in the ground states $(T=0)$.

Thus, in terms of the respective binding energies B, Q_{eff} is defined as

$$Q_{eff}(T) = B(T) - [B_1(T=0) + B_2(T=0)]$$

$$= TKE(T) = V(R_a) \tag{2.6}$$

Since, $R_a = C_t(\eta)$ for $T=0$, $\Delta R(\eta)$ corresponds to the change in TKE at T with respect to its value at $T=0$, and hence can be estimated exactly for the temperature effects in the scattering potential $V(R)$.

At temperature T, the preformation factor P_0 in Eq. (2.4) is calculated at $R_a = C_t(\eta) + \overline{\Delta R}$, with the temperature effects also included in $\psi(\eta)$ through a Boltzmann-like function,

$$|\psi|^2 = \sum_{\nu=0}^{\infty} \left|\psi^{\nu}\right|^2 \exp(-E^{\nu}/T), \tag{2.7}$$

with the compound nucleus temperature T (in MeV) related as

$$E^*_{CN} = \left(\frac{A}{9}\right)T^2 - T\,; \tag{2.8}$$

and for the penetrability P, Eqs. (2.6) for each η and T values mean that

$$V(R_a) = V(C_t + \overline{\Delta R}) = V(R_b) = Q_{eff}(\overline{\Delta R}) = TKE(T) \tag{2.9}$$

with R_b as the second turning point.

The penetrability P is calculated as the WKB tunneling probability, solved analytically in Ref. 2 and 3.

$$P = \exp[-\frac{2}{\hbar}\int_{R_a}^{R_b}\{2\mu[V(R)-Q_{eff}]\}^{1/2}dR] \tag{2.10}$$

The fragmentation potential $V_R(\eta,T)$ at any temperature T, in Eq. (2.3), is calculated within the Strutinsky renormalization procedure, as

$$V_R(\eta,T) = \sum_{i=1}^{2}[V_{LDM}(A_i,Z_i,T)] + \sum_{i=1}^{2}[\delta U_i]\exp(-T^2/T_0^2) + E_c(T) + V_P(T) + V_l(T) \tag{2.11}$$

where the T-dependent liquid drop energy $V_{LDM}(T)$ is that of Ref. 10, with (Seeger's) constant at $T=0$ refitted to give binding energies of[11,] defined as $B = V_{LDM}(T=0) + \delta U$. The shell corrections are calculated in the "empirical method" of Myers and Swiatecki[12].

The V_P is an additional attraction due to the nuclear proximity potential[13,] which is also considered temperature dependent here,

$$V_P(R,T) = 4\pi\overline{R}(T)\gamma b(T)\phi(s,T), \tag{2.12}$$

where $\overline{R}(T)$ and $\phi(s,T)$ are, respectively, the inverse of the root mean square radius of the Gaussian curvature and the universal function, which is independent of the geometry of the system, given by

$$\phi(s,T) = \begin{cases} -\frac{1}{2}(s-2.54)^2 - 0.0852(s-2.54)^3 \\ -3.437\exp(-s/0.75) \end{cases} \tag{2.13}$$

for $s \le 1.2511$ and $s \ge 1.2511$ respectively,

$$\overline{R}(T) = \frac{C_1(T)C_2(T)}{C_t(T)} \tag{2.14}$$

and γ is the specific nuclear surface tension given by

$$\gamma = 0.9517\left[1 - 1.7826\left(\frac{N-Z}{A}\right)^2\right] \text{MeV fm}^{-2} \tag{2.15}$$

In Eq. (2.12), $s(T)(=[R - C_t(T)]/b(T)$ is the overlap distance, in units of b, between the colliding surfaces. The temperature dependence in radii R_i is given as[10, 14]

$$R_i(T) = r_0(T)A_i^{1/3} = 1.07(1 + 0.01T)A_i^{1/3} \tag{2.16}$$

with the surface width

$$b(T) = 0.99(1 - 0.99T^2) \tag{2.17}$$

The same temperature dependence of $R(T)$ is also used for Coulomb potential $E_c(T) = Z_1 Z_2 e^2 / R(T)$, where the charges Z_i are fixed by minimizing the potential $V_R(\eta, T)$ in the charge asymmetry coordinate $\eta_Z = (Z_1 - Z_2)/(Z_1 + Z_2)$. The shell corrections δU in the Eq. (2.11) are considered to vanish exponentially for $T_0 = 1.5$ Mev.[15]

Also, for the angular momentum effects

$$V_l(T) = \frac{\hbar^2 l(l+1)}{2I(T)}. \tag{2.18}$$

In the nonsticking limit, where $R_a = C_1(T) + C_2(T) + \Delta R = C_t(T) + \Delta R$, the moment of inertia in Eq. (2.18) is given by

$$I(T) = I_{NS}(T) = \mu R_a^2. \tag{2.19}$$

In this case, the separation distance ΔR is assumed to be beyond the range of nuclear proximity forces, which is about 2 fm. However, when it is within the range of nuclear proximity (<2 fm), we get in the complete sticking limit

$$I(T) = I_s(T) = \mu R_a^2 + \frac{2}{5} A_1 m C_1^2 + \frac{2}{5} A_2 m C_2^2 . \qquad (2.20)$$

For the l value, in terms of the bombarding energy $E_{c.m.}$ of the entrance channel η_{in} , we have

$$l = l_c = R_a \sqrt{2\mu[E_{c.m.} - V(R_a, \eta_{in}, l = 0)]} / \hbar . \qquad (2.21)$$

The mass parameters $B_{\eta\eta}(\eta)$, representing the kinetic energy part in Eq. (2.3), are the smooth classical hydrodynamical masses[16], since at high temperatures the shell effects are almost completely washed out.

Finally, the temperature-dependent scattering potential $V(R,T)$, normalized to exit channel binding energy, is

$$V(R,T) = Z_1 Z_2 e^2 / R(T) + V_P(T) + V_l(T) \qquad (2.22)$$

This means that all the energies are measured with respect to $B_1(T) + B_2(T)$, and the fragments go to ground state $(T \to 0)$ via the emission of light particle(s) and/or $\gamma-$rays of energy E_x .

2.2.1 Oriented Collisions

For the deformation and orientation effects we use the model developed at Chandigarh by Gupta and collaborators[2, 3].

The potential V for orientated nuclei is the sum of two binding energies B_i and deformation and orientation dependent Coulomb and proximity potentials:

$$V(\eta, R) = -\sum_{i=1}^{2} B_i(A_i, Z_i, \beta_{\lambda i}) + E_C(Z_i, \beta_{\lambda i}, \theta_i) + V_P(A_i, \beta_{\lambda i}, \theta_i) \tag{2.23}$$

The Coulomb and proximity potentials with higher multipole deformations included, are obtained respectively

$$E_C = \frac{Z_1 Z_2 e^2}{R} + 3Z_1 Z_2 e^2 \sum_{\lambda, i=1,2} \frac{1}{2\lambda+1} \frac{R_{0i}^{\lambda}}{R^{\lambda+1}} Y_{\lambda}^{(0)}(\alpha_i) \left[\beta_{\lambda i} + \frac{4}{7} \beta_{\lambda i}^2 Y_{\lambda}^{(0)}(\alpha_i) \delta_{\lambda,2} \right] \tag{2.24}$$

with $R_i(\alpha_i) = R_{0i}\left[1 + \sum_{\lambda} \beta_{\lambda i} Y_{\lambda}^{(0)}(\alpha_i)\right]$ and $R_{0i} = 1.28A_i^{1/3} - 0.78 + 0.8A_i^{-1/3}$

The nuclear proximity potential is given as,

$$V_P = 4\pi \overline{R} \gamma b \phi(s_0) \tag{2.25}$$

where the surface energy coefficient $\gamma = 0.9517\left[1 - 1.78269(N-Z)^2 / A^2\right]$ MeV fm^{-1} ; the surface thickness $b \approx 1$fm; $\overline{R}$ is the mean curvature radius given as; $\frac{1}{\overline{R}^2} = \frac{1}{R_{11}R_{12}} + \frac{1}{R_{21}R_{22}} + \frac{1}{R_{11}R_{22}} + \frac{1}{R_{21}R_{12}}$ where the four principal radii of curvature R_{i1} and R_{i2} at the points D and E of minimum s_0, are given by Eq. (15) in Ref. 3, and the universal function, independent or the geometry of nuclear system, is

$$\phi(s_0, T) = \begin{cases} -\frac{1}{2}(s_0 - 2.54)^2 - 0.0852(s_0 - 2.54)^3 \\ -3.437\exp(-s_0 / 0.75) \end{cases} \tag{2.26}$$

Where s_0 is the shortest distance between the colliding surfaces, parallel to R, taken along the collision axis, in units of b, and defined as;

$s_0 = [R - R_1(\alpha_1)\cos\psi_1 - R_2(\alpha_2)\cos\psi_2]/b$; ψ_i are the angles that R_i make with s_0 as shown in the figure 2.1. For s_0 to be minimum, i.e. $\partial s_0 / \partial \alpha_i = 0$, it follows from figure 2.1 that $\psi_1 = \theta_1 - \alpha_1$, $\psi_2 = 180 - \theta_2 - \alpha_2$ and $\tan\psi_i = -R_i'(\alpha_i)/R_i(\alpha_i)$. The figure 2.1 shows the schematic configuration of two axially symmetric deformed, oriented nuclei, lying in the same plane.

2.3 Quantum Mechanical Fragmentation Theory

In QMFT[17-30], the essential quantities for the description of the nuclear dynamics are the potential energy surfaces and the mass parameters defining the kinetic energy of the system while the static properties of nuclear system are determined by the potential energy only. The QMFT is worked out in terms of the following collective variables:

(1) Relative separation coordinate R between the two nuclei or, in general, two fragments (or, equivalently, the length parameter $\lambda = L/2R_0$, with L as the length of the nucleus and R_0 as the radius of an equivalent spherical nucleus).

(2) The orientation degrees of freedom θ_i (i=1, 2) of the deformed nuclei.

(3) The deformation co-ordinates $\beta_{\lambda i}$ (λ=2, 3.4... and i =1, 2) of the colliding nuclei.

(4) Azimuthal angle ϕ between the principal planes of the two colliding nuclei.

(5) Neck parameter ε, defined by the ratio $\varepsilon = E_0/E'$ for the interaction region ($R \prec R_1 + R_2, R_i (i = 1,2)$ is the radius of the two nuclei);

Where E_0 is the actual height of the barrier and E' is the fixed barrier of the two center oscillator. $\varepsilon = 0$ represents a broad neck formation, whereas $\varepsilon = 1$ gives that the neck is fully squeezed in, corresponding to the asymptotic region $(R \succ R_1 + R_2)$.

(6) Mass and charge fragmentation co-ordinates.[17, 18, 29]

For two body channels, the mass and charge fragmentations for separated nuclei/fragments are defined by the mass and charge–asymmetry coordinates as

$$\eta = \frac{A_1 - A_2}{A}; \qquad \eta_Z = \frac{Z_1 - Z_2}{Z} \tag{2.27}$$

Similarly, the neutron asymmetry coordinate[18]

$$\eta_N = \frac{N_1 - N_2}{N} \tag{2.28}$$

can also be used, but it is sufficient to treat only two of them as dynamical co-ordinates since they are related as

$$\eta = \frac{Z\eta_Z}{A} + \frac{N\eta_N}{A} \tag{2.29}$$

Here $A = A_1 + A_2$, $Z = Z_1 + Z_2$ and $N = N_1 + N_2$. A_i, Z_i and N_i are respectively the mass number, the charge number and the neutron number of two fragments. A, Z and N are respectively the mass number, the charge number and neutron number of the compound system. The limiting values of η are $0 \le |\eta| \le 1$ and thus allows a unified description of a few nucleon or multi nucleon (a cluster) transfer, a large mass transfer, the complete fusion ($|\eta| = 1$) of nuclei and the symmetric ($\eta = 0$), asymmetric and super symmetric fission of a nucleus or compound nucleus. The η_Z coordinate gives the associated charge distribution effects. In terms of these collective coordinates and their velocities, the collective Hamiltonian can be written as (taking β to stand for $\beta_{\lambda 1}$ and $\beta_{\lambda 2}$ (β=2, 3, 4....)).

$$H = K(R, \beta, \varepsilon, \eta, \eta_z; \dot{R}, \dot{\beta}, \dot{\varepsilon}, \dot{\eta}, \dot{\eta_z}) + V(R, \beta, \varepsilon, \eta, \eta_z). \tag{2.30}$$

For the compound nucleus formation, the neck parameter $\varepsilon = 0$ is assumed, since once the neck formation starts between the two colliding nuclei, then fission phenomenon takes place, i.e. excited compound nucleus will proceed towards the disintegration process.

For the potential $V(\eta,\eta_z,R)$, minimized in the η_z co-ordinate, Schrodinger wave equation in terms of the mass parameters η and relative separation R co-ordinates can be written as:

$$H(\eta,R)\Psi(\eta,R) = E(\eta,R)\Psi(\eta,R) \tag{2.31}$$

With the Hamiltonian,

$$H(\eta,R) = K(\eta) + K(R) + K(\eta,R) + V(\eta) + V(R) + V(\eta,R) \tag{2.32}$$

Here, K refers to the kinetic energy and V to the collective potential energy. The mass parameters B_{ij}, defining the kinetic energy term K in the above Eqs. (2.30) and (2.32) are either the consistently calculated cranking masses using the Asymmetric Two-Center Shell Model (ATCSM) or the classical hydrodynamical masses, which are shown to have good agreement with microscopic cranking calculations. The coupling term of the kinetic energy K(η,R), proportional to $\frac{\partial^2}{\partial\eta\partial R}$, is neglected here, since the coupled cranking masses are very small[17,18] ($B_{R\eta} << (B_{RR}B_{\eta\eta})^{1/2}$ and $B_{R\eta_Z} << (B_{RR}B_{\eta_Z\eta_Z})^{1/2}$). Same is true for the coupling term of potential energy $V(\eta,R)$. Therefore, in a decoupled approximation[30], the Schrodinger equation (2.31) can be solved for which the Hamiltonian takes the form:

$$\mathrm{H} = -\frac{\hbar^2}{2\sqrt{B_{\eta\eta}}}\frac{\partial}{\partial\eta}\frac{1}{\sqrt{B_{\eta\eta}}}\frac{\partial}{\partial\eta} - \frac{\hbar^2}{2\sqrt{B_{RR}}}\frac{\partial}{\partial R}\frac{1}{\sqrt{B_{RR}}}\frac{\partial}{\partial R} + V(\eta) + V(R) \tag{2.33}$$

For decoupled Hamiltonian (2.33), Schrodinger wave equation (2.31) can be separated for the two co-ordinates η and R as follows,

$$\left\{-\frac{\hbar^2}{2\sqrt{B_{\eta\eta}}}\frac{\partial}{\partial\eta}\frac{1}{\sqrt{B_{\eta\eta}}}\frac{\partial}{\partial\eta} + V(\eta)\right\}\psi^{\nu}(\eta) = E\eta^{\nu}\psi^{\nu}(\eta) \tag{2.34}$$

and

$$\left\{-\frac{\hbar^2}{2\sqrt{B_{RR}}}\frac{\partial}{\partial R}\frac{1}{\sqrt{B_{RR}}}\frac{\partial}{\partial R} + V(R)\right\}\psi^{\nu}(R) = ER^{\nu}\psi^{\nu}(R) \tag{2.35}$$

With $$\Psi(\eta, R) = \Psi(\eta)\Psi(R) \tag{2.36}$$

and $$E = E_\eta + E_R \tag{2.37}$$

The states $\Psi^\upsilon(\eta)$ are the vibrational states in the potential V (η) and are labeled by the quantum numbers υ = 0, 1, 2…

On solving Eq. (2.6) numerically, $\left|\Psi^\nu(\eta)\right|^2$ gives the probability P_0 of finding the mass fragmentation η at a fixed R on the decay path.

$$P_0(A_2) \propto \left|\Psi^\nu(A_2)\right|^2 \tag{2.38}$$

For fission studies, like the spontaneous fission and fission through the barrier, the motion in R at the saddle point is adiabatically slow as compared to the η motion.

2.3.1 The Scattering Potential V(R)

For a fixed η i.e. for a given outgoing fragment (A_1, A_2) combination, the scattering potential V(R) is defined as the sum of the deformations, orientations dependant coulomb potential, proximity potential and angular momentum dependant potential, i.e.

$$V(R) = V_c(R, Z_i, \beta_{\lambda i}, \theta_i, \phi) + V_p(R, A_i, \beta_{\lambda i}, \theta_i, \phi) + V_l(R, A_i, \beta_{\lambda i}, \theta_i, \phi) \tag{2.39}$$

For co-planar nuclei, $\Phi = 0^0$, and for spherical-plus-deformed nuclear collisions, only one orientation angle θ is enough, referring to the rotationally-symmetric deformed nucleus.

2.3.2 The Fragmentation Potential V (η)

The collective potential energy or the fragmentation potential $V(\eta, R)$, is calculated as,

$$V(\eta,R) = -\sum_{i=1}^{2}[B_i(A_i,Z_i,\beta_{\lambda i})] + V_c(R,Z_i,\beta_{\lambda i},\theta_i,\phi) + V_p(R,A_i,\beta_{\lambda i},\theta_i,\phi) + V_l(R,A_i,\beta_{\lambda i},\theta_i,\phi) \quad (2.40)$$

Here B_i (i=1, 2) are the binding energies of the two nuclei, available from the experimental data of Audi-Wapstra[33]. Wherever the experimental B's are not available, the theoretical binding energies of Moller et al.[34] are used. Note that the binding energies contain both the macroscopic (liquid drop part) and the microscopic (shell correction) part.

The fragmentation potential V (η) is calculated at a fixed distance R = R1 +R2 + δR or R = C1 + C2 + δC fm, with C_i (i=1, 2) as the Sussmann central radii related to the radius vector R_i as $C_i = R_i\left(1 - \frac{b^2}{R_i^2}\right)$ with

$$R_i = R_{0i}\left[1 + \sum_{\lambda}\beta_{\lambda i}Y_{\lambda}^{(0)}(\alpha_i)\right] \quad (2.41)$$

and

$$R_{0i} = 1.28A_i^{1/3} - 0.76 + 0.8A_i^{-1/3} \quad (2.42)$$

Here λ=2, 3, 4... and α_i is an angle that the radius vector R_i of the colliding nuclei makes with the symmetry axis(see Figure. 2.1) .The diffuseness of the nuclear surface (i.e. the surface thickness) b=0.99 fm. The charges Z_i are fixed by minimizing the potential V (η) in the η_Z coordinate at each η value.

For the study of excited systems, where the nuclear temperature effects also come into picture, the fragmentation potential at fixed R is

$$V(\eta,T) = \sum_{i=1}^{2}V_{LDM}(A_i,Z_i,T) + \sum_{i=1}^{2}\delta U\exp\left(-\frac{T^2}{T_0^2}\right) + V_c(Z_i,\beta_{\lambda i},\theta_i,\phi,T) + V_p(A_i,\beta_{\lambda i},\theta_i,\phi,T) + V_l(A_i,\beta_{\lambda i},\theta_i,\phi,T) \quad (2.43)$$

Here, V_{LDM} (A_i, Z_i, T) is the liquid drop part of the binding energy and δU, the shell corrections. Note that the calculation of fragmentation potential involves all the possible decay channels and the number of all such possible decay channels becomes more

and more with the increasing mass of the mother nucleus. The nuclear temperature T (in MeV) is related to the excitation energy E^*_{CN} of the compound nucleus, through a semi-empirical statistical relation as:

$$E^*_{CN} = \frac{1}{10} AT^2\text{-}T \qquad \text{(MeV)} \qquad (2.44)$$

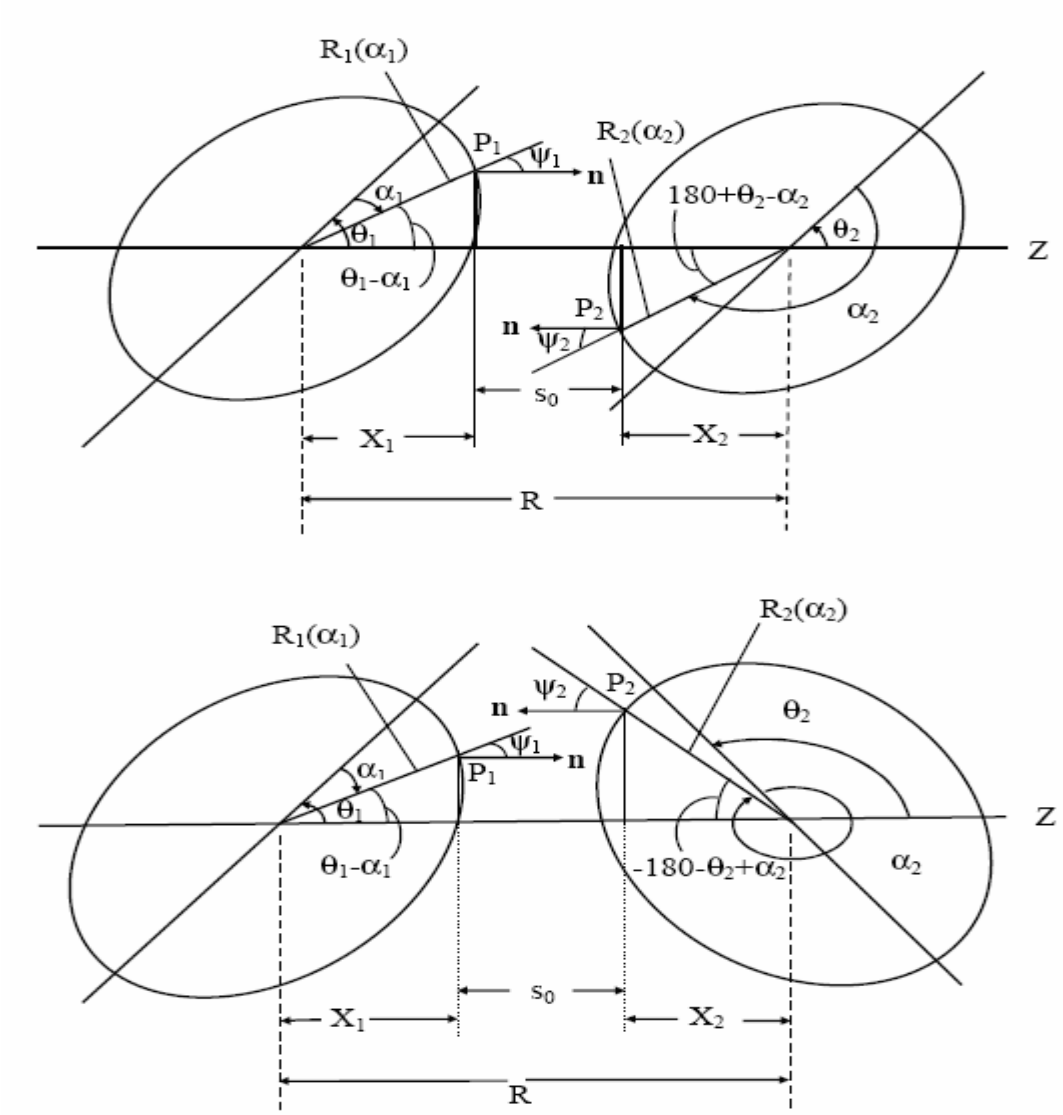

Figure 2.1: Schematic configurations of two (equal/ unequal) axially symmetric deformed, oriented nuclei, lying in the same plane and for various θ1 and θ2 values in the range 0^0 to 180^0. The θ's are measured in anti-clockwise from the colliding axis and the angle α's in clockwise from the symmetry axis.

The shell corrections δU in Eq. (2.4) are considered to vanish exponentially for $E^*_{CN} \geq$ 60 MeV, giving T_0 = 1.5 MeV. At higher excitation energies the shell corrections vanish

completely and only the liquid drop part of energy is present. The shell corrections play an important role in determining or empirical fitting of nuclear masses, because the nuclear masses calculated by using the smooth liquid drop formula show large deviations with respect to the experimental masses. It means that in the experimental masses there exist deep minima at specific neutron and/or proton numbers indicating the presence of shell structure, the so-called magic numbers in nuclei.

This characteristic behavior cannot be reproduced by the liquid drop part alone, which means that the introduction of microscopic shell correction in the mass formula is essential. Thus, shell corrections accounts for the removal of deviation from the liquid drop calculations (uniform distribution of nucleons), and are defined, within Strutinsky[31] method as

$$\delta \mathrm{U} = \mathrm{U} - \tilde{U} \tag{2.45}$$

where, $\mathrm{U} = \sum_{\nu} E_{\nu} 2n_{\nu}$ is the sum over all occupied single particle states and

$$\tilde{U} = 2 \int_{-\infty}^{\tilde{\lambda}} E \, \tilde{g}(E) dE \tag{2.46}$$

is the average energy for uniform distribution. In general, the microscopic shell correction, together with the liquid drop part, gives a proper description of the binding energy of the nucleus. This method, however, does not give a proper description of light mass nuclei. The difficulty is the inadequacy of shell model for very light nuclei. For this reason, the macro-microscopic calculations of Moller et al.[34] are tabulated for Z ≥8 only. For Z ≤ 8, one could alternatively use the empirical shell correction method of Myers-Swiatecki[35] which again is not very satisfactory for light nuclei (Z ≤ 16). Gupta and collaborators[2, 3] have modified this empirical method and obtained a better description of the shell corrections for the light as well as heavy mass region, i.e., 1 ≤Z ≤118[32].

2.4 The Preformed Cluster-decay Model for ground state decay of nucleus

These models fall into two main categories:

(i) Unified Fission models (UFM), and

(ii) Preformed cluster-decay models (PCM).

In the *UFM*, the cluster decay is dealt simply as a barrier penetration problem where as the preformed cluster model (PCM) distinguishes itself from the unified fission model (UFM) in its basic assumption of the emitted cluster(s) being preborn in the parent nucleus with a probability that decreases with the increasing size of the cluster. This suggests that the process of cluster decay will stop somewhere and that of fission will take over, with a possible overlap for some region. It is seen that such an overlap does exist indeed for clusters of masses $42 < A_2 < 50$.

The PCM is developed as a further modification of the Gamow theory, considering not only the penetration of a realistic barrier (coulomb + nuclear, as in UFM), but also associating a preformation probability P_0 to the emitting cluster.

The Preformed Cluster model (PCM) Of Gupta and collaborators[36-39], with effects of deformation and orientation degrees of freedom included, is based on the well-known quantum mechanical fragmentation theory (QMFT) [17-30]. In PCM, the clusters are considered to be pre-born in the parent nucleus before penetrating the interaction barrier. The model is worked out in term of only one parameter, the neck length parameter ΔR, assimilating the neck formation effects of the two-centre shell –model shape. The decay constant and hence the decay half-life time in PCM is defined as in Eq. (2.1).

$$\lambda^{PCM} = \upsilon_0 P P_0, \qquad T_{1/2} = \ln 2/\lambda$$

Here υ_0 is the impinging frequency with which the cluster hits the barrier, given by

$$\upsilon_0 = \upsilon/R_0 = \frac{(2E_2/\mu)^{1/2}}{R_0} \qquad (2.47)$$

where R_0 is the radius of parent nucleus and $E_2 = ½\ \mu\ v^2$ is the kinetic energy of the emitted cluster. The impinging frequency υ_0 is nearly constant~ 10^{21} s^{-1} for all the observed cluster decays. since both the emitted cluster and daughter nuclei are produced in ground state, the entire positive Q-value of decay is the total kinetic energy, ($Q = E_1 + E_2$), available for the decay process, which is shared between the two fragments, such that for the emitted cluster,

$$E_2 = \frac{A_1}{A}Q \qquad (2.48)$$

and, E_1 (=$Q - E_2$) is the recoil energy of daughter nucleus. P_0 is preformation probability of the cluster, and P is the WKB penetration probability of cluster through the barrier, calculated within the QMFT.

The QMFT is worked out in terms of the collective coordinates of mass and charge asymmetries

$$\eta = \frac{A_1 - A_2}{A_1 + A_2} \qquad \text{and} \qquad \eta_z = \frac{Z_1 - Z_2}{Z_1 + Z_2},$$

(1 and 2 stand, respectively, for daughter and cluster) and the relative separation R, to which are added the multipole deformations $\beta_{\lambda i}$ and orientations θ_i (i=1, 2) of daughter and cluster nuclei. In PCM, the two coordinates η and R refer, respectively, to the nucleon-division (or-exchange) between the daughter and cluster, and the transfer of positive Q-value to the total kinetic energy ($E_1 + E_2$) of two nuclei as they are produced in the ground state, as already pointed out above.

The preformation probability P_0 (A_i) (≡ | Ψ (η (A_i)) |^2, i=1 or 2) is the solution of the stationary Schrodinger equation in η, at fixed R =R_a, the first turning point of the penetration path used for calculating the penetrability P (see figure.2.2). Thus, the structure information of the compound nucleus is contained in P_0 via the fragmentation potential.

$$V_R(\eta) = -\sum_{i=1}^{2}[B_i(A_i, Z_i)] + V_c(R, Z_i, \beta_{\lambda i}, \theta_i) + V_p(R, A_i, \beta_{\lambda i}, \theta_i) + V_l(R, A_i, \beta_{\lambda i}, \theta_i) \quad (2.49)$$

used in the above said stationary Schrodinger equation. Here, $B_i(A_i, Z_i)$ are the ground state binding energies from Ref. 40, and V_c, V_p, and V_l are, respectively, the Coulomb, nuclear proximity, and angular- momentum dependant potentials. For ground-state decays, l=0 is a good approximation.

In Eq. (2.49), the proximity potential V_p for deformed and oriented nuclei is given as,

$$V_P(s_0) = 4\pi \bar{R} \gamma b \phi(s_0) \quad (2.50)$$

With the specific nuclear surface tension coefficient γ = 0.9517 [1- 1.7826 $\left(\frac{N-Z}{A}\right)^2$] MeV fm^{-2}, the surface thickness b =0.99 fm, and the universal, function, independent of the geometry of nuclear system as given by Eq. (2.26).

The mean curvature radius in Eq. (2.50) for two co-planar nuclei is

$$\frac{1}{\bar{R}^2} = \frac{1}{R_{11}R_{12}} + \frac{1}{R_{21}R_{22}} + \frac{1}{R_{11}R_{22}} + \frac{1}{R_{21}R_{12}} \quad (2.51)$$

with the four principal radii of curvature R_{i1} and R_{i2} of the two reaction partners given by Eq. (4) of Ref. 42, and the radius vectors

$$R_i(\alpha_i) = R_{0i}\left[1 + \sum_{\lambda} \beta_{\lambda i} Y_{\lambda}^{(0)}(\alpha_i)\right] \quad (2.52)$$

with the R_{0i} given by

$$R_{0i} = 1.28A_i^{1/3} - 0.76 + 0.8A_i^{-1/3} \tag{2.53}$$

For Coulomb interaction extended Wong is[43] expression for two non-overlapping charge distributions, to all higher multipole deformations (λ=2, 3, 4...), is [41]

$$V_C = \frac{Z_1 Z_2 e^2}{R} + 3Z_1 Z_2 e^2 \sum_{\lambda,i=1,2} \frac{1}{2\lambda+1} \frac{R_i^{\lambda}(\alpha_i)}{R^{\lambda+1}} Y_{\lambda}^{(0)}(\theta_i) \left[\beta_{\lambda i} + \frac{4}{7} \beta_{\lambda i}^2 Y_{\lambda}^{(0)}(\theta_i) \right] \tag{2.54}$$

The mass parameters $B_{\eta\eta}$ (η), entering the P_0 calculation via the kinetic energy term, are the smooth classical hydrodynamical masses[44], used for reasons of simplicity. The penetrability P in (1) is the WKB integral between R_a and R_b, the first and second turning points, respectively (Fig. 2.2). In other words, the tunneling begins at R= R_a and terminates at R=R_b, with V(R_b)=Q-value for ground state decay.

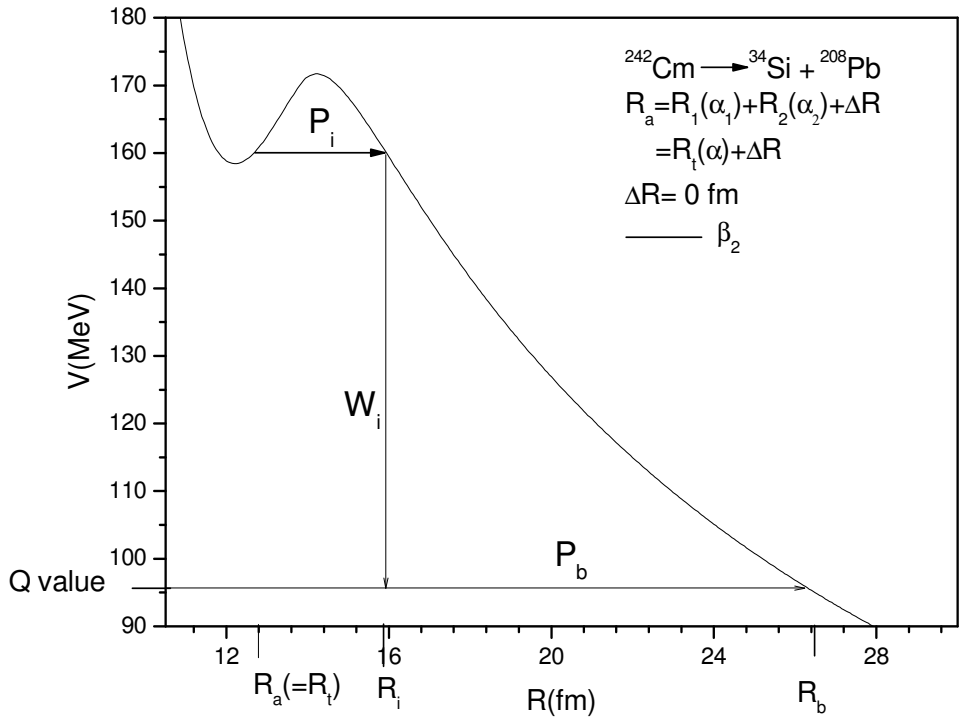

Figure.2.2: The scattering potentials for the ^{34}Si cluster decay of parent nucleus ^{242}Cm, i.e. ^{242}Cm→^{34}Si + ^{208}Pb, for ^{34}Si considered as a deformed nucleus.

Thus, as per Fig.2.2, the transmission probability P consists of the following three contributions[36, 37]

1. The penetrability P_i from R_a to R_i,

2. The (inner) de-excitation probability W_i at R_i, and

3. The penetrability P_b from R_i to R_b.

giving the penetration probability as

$$P = P_i W_i P_b \tag{2.55}$$

The shifting of first turning point from R_a to R_0, the compound nucleus radius, gives the penetrability P similar to that of Shi and Swiatecki[45] for spherical nuclei, which is known not to fit the experimental data without the adjustment of assault frequency. Following the excitation model of M.Greiner and W. Scheid[46] , we take the de-excitation probability W_i=1 for a heavy cluster decays, which reduces Eq.(2.55) to the following:

$$P = P_i P_b , \tag{2.56}$$

Where P_i and P_b in WKB approximation are

$$P_i = \exp\left[-\frac{2}{\hbar} \int_{R_a}^{R_{ii}} \{2\mu[V(R) - V(R_i)]\}^{1/2} dR \right] \tag{2.57}$$

and

$$P_b = \exp\left[-\frac{2}{\hbar} \int_{R_i}^{R_b} \{2\mu[V(R) - Q]\}^{1/2} dR \right] \tag{2.58}$$

For the first turning point, we use the following postulate

$$R_a(\eta) = R_1(\alpha_1) + R_2(\alpha_2) + \Delta R$$

$$= R_t(\alpha, \eta) + \Delta R \qquad (2.59)$$

where the η- dependence of R_a is contained in R_t, and ΔR is a parameter, assimilating the neck formation effects of two centre shell model[38]. This method of introducing the neck-length parameter ΔR is also used in our dynamical cluster-decay model (DCM) [1-16] and in the scission-point[47] and saddle-point[48, 49] (statistical) fission models for decay of a hot and rotating compound nucleus.

References

1. R.K. Gupta, R. Kumar, N.K. Dhiman, M. Balasubramaniam, W. Scheid, and C. Beck, Phys. Rev. C **68,** 014610 (2003); M. Balasubramaniam, R. Kumar, R.K. Gupta, C. Beck, and W. Scheid, J. Phy. G: Nucl. Part. Phys. **29,** 2703 (2003)

2. R.K Gupta Proc. 5th Int. conf. on Nuclear Reaction Mechanisms, Varenna, P **416** (1988)

3. S Malik and R K Gupta Phys. Rev. C **39,** 1992 (1989).

4. J. Maruhn and W. Greiner, Phys. Rev. Lett. **32**, 548 (1974)

5. R.K Gupta, W. Scheid, and W. Greiner, Phys. Rev. Lett. **35**, 353 (1975)

6.R.K Gupta and W. Greiner, Heavy Elements and Related New Phenomena, World Scientific, Singapore, edited by W. Greiner and R.K Gupta, Vol. **I**, P 397; P 536 (1999)

7. D R Saroha and R.K Gupta, J. Phy. G 12**,** 1265 (1986)

8. S. Kumar and R.K Gupta, Phys. Rev. C **55**, 218 (1997)

9. R.K Gupta, M. Balasubramaniam, C. Mazzocchi, M. La Commara, and W. Scheid, Phys. Rev. C **65** 024601 (2002).

10. N.J. Davidson, S.S. Hsiao, J. Markram, H.G. Miller, and Y. Tsang, Nucl. Phys. **A570**, 61C (1994).

11. G. Audi and A.H. Wapstra, Nucl. Phys. **A595**, 4 (1995)

12. W. Myers and W.J. Swiatecki, Nucl. Phys. **A81**, 1 (1966)

13. J. Blocki, J. Randrup, W.J. swiatecki, and C.F Tsang, Ann. Phys. (NY) **105**, 427 (1977)

14. G. Royer and J. Migner, J. Phy. G **18,** 1781 (1992), and earlier references therein.

15. A.S Jensen and J. Damgaard, Nucl. Phys. **A203**, 578 (1973)

16. H Kroeger and W Scheid, J. Phys. G: Nucl. Phys. **6,** L85 (1980)

17. J. Maruhn and W. Greiner, Phys. Rev. Lett. 32, 548 (1974).

18. R.K. Gupta, W. Scheid and W. Greiner, Phys. Rev. Lett. 35, 353 (1975)

19. A. Sandulescu, R.K. Gupta, W. Scheid and W. Greiner, Phys. Lett. 60B, 225 (1976).

20. R.K. Gupta, A. S˘andulescu and W. Greiner, Phys. Lett. 67B, 257 (1977); Rev. Roum. Phys. 23, 51 (1978)

21. S.Yamaji, W. Scheid, H.J. Fink and W. Greiner, Z. Phys. A 278, 69 (1976)

22. S. Yamaji, W. Scheid, H.J. Fink and W. Greiner, J. Phys. G: Nucl. Phys. 2, L189 (1976)

23. S. Yamaji, K.H. Ziegenhain, H.J. Fink, W. Greiner and W. Scheid, J. Phys. G: Nucl. Phys. 3, 1283 (1977)

24. R.K. Gupta, A. Sandulescu and W. Greiner, Z. Naturforsch. 32a, 704 (1977)

25. R. K. Gupta, C. Pirvulescu, A. Sandulescu and W. Greiner, Z. Phys. A 283, 217 (1977); Sovt. J. Nucl. Phys. 28, 160 (1978)

26. R.K. Gupta, Z. Physik. A 281, 159 (1977)

27. A. Sandulescu, H.J. Lustig, J. Hahn, and W. Greiner, J. Phys. G: Nucl. Phys. 4, L279 (1978)

28. H.J. Lustig, J.A. Maruhn, and W. Greiner, J. Phys. G: Nucl. Phys. 6, L25 (1980).

29. H.J. Fink and W. Greiner and R.K. Gupta and S. Liran and J.H. Maruhn and W. Scheid and O. Zohni, in Proceedings of Int. Conf. on Reaction between Complex Nuclei, Nashville, 1974, 21, (Amsterdam: North Holland), pages 2.

30. R. K. Gupta, IANCAS Bull. (India), 6, 2(1990)

31.V. M. Strutinsky, Nucl. Phys. A 95, 420 (1967)

32. M. Balasubraniam, R. Kumar, R.K. Gupta, C. Beck, and W. Scheid, J. Phys. G 29, 2703 (2003): R.K. Gupta, M.K. Sharma and B. Singh, Phys. Rev. C-to be published

33. G. Audi and A.H. Wapstra, Nucl. Phys. A 595,4 (1995).

34. P. Moller, J. R. Nix, W. D. Myers,and W. J. Swiatecki, At. Data Nucl. Data

Tables 59, 185 (1995)
35. W. Myers and W.J. Swiatecki, Nucl. Phys. 81, 1 (1966)
36. R.K. Gupta, in Proc. 5th Int. Conf. on Nuclear Reaction Mechanisms, Varenna, edited by E. Gadioli (Ricerca Scientifica ed Educazione Permanente, Milano) (1988), p.146
37. S.S Malik and R.K. Gupta, Phys. Rev. C 39, 1992 (1989)
38. S. Kumar and R.K. Gupta, Phys.Rev.C 55, 218 (1997)
39. R.K. Gupta, in Heavy Elements and Related New Phenomena, Vol. II, Edited by W. Greiner and R.K. Gupta, (World Scientific, Singapore) (1990), p.731
40. P.Moller, J.R. Nix, W.D. Myers, and W.J. Swiatecki, At. Data Nucl. Data Tables 59, 185 (1995)
41. R.K Gupta, M. Balasubramaniam, R.Kumar, N.Singh, M.Mahhas, and W.Greiner, J.Phys. G: Nucl. Part. Phys. 31, 631 (2005)
42. R.K. Gupta, N.Singh, and M.Mahhas, Phys.Rev. 70, 034608 (2004)
43. C.Y. Wong, Phy.Rev.Lett.31, 766 (1973)
44. H. Kroger and W. Scheid, J. Phys. G 6, L85 (1980)
45. Y.J. Shi and W.J. Swiatecki, Phys.Rev. C 54, 300 (1985)
46. M. Greiner and W. Scheid, J.Phys. G: Nucl.Phys. 12, L 229 (1986)
47. T. Matsuse, C. Beck, R. Nouicer, and D. Mahboub, Phys.Rev.C 55,1380 (1997)
48.S.J. Sanders, D.G. kover, B.B.Back, C.Beck, D.J. Henderson, R. V.F. Janssens, T.F. wang, and B.D. Wilkins, Phys. Rev. C 40, 2091 (1989)
49. S.J. Sanders, Phys.Rev.C 44, 2676 (1991)

Chapter 3

CALCULATIONS AND DISCUSSION OF THE RESULTS

3.1 Calculations and discussion of the results

In the present work, we intend to investigate the role of deformation and orientations of the decaying parent nucleus along with that of emitted fragment(s) and corresponding daughter nucleus in the ground state decay using the preformed cluster model (PCM) of Gupta and collaborators. The study is limited to only those clusters in which daughter formed is always a Pb isotope (with Z=82) and its nearby nuclei with even mass number. It is relevant to mention here that all the parents ^{228,230}Th, ^{232,234,238}U, ^{236,238}Pu and ^{242}Cm and their respective emitted clusters ^{20}O, ^{24}Ne and ^{28,30}Mg considered here are deformed, except for ^{25,26}Ne and ^{32,34}Si which are spherical/nearly spherical. Also all parent nuclei are prolate deformed whereas clusters ^{24}Ne, ^{30}Mg are oblate deformed and ^{20}O, ^{28}Mg are prolate deformed. Another point of interest to note may be that all the parent nuclei have almost the similar N/Z ratio.

It is extremely interesting to note that in the domain of Preformed cluster decay model (PCM), not only the shapes of the parent, daughter and cluster are important, but also the shapes of all other possible fragmentations of the decaying parent nucleus are important via the calculation of fragmentation potential, and hence the preformation factor P_0. We shall see that the inclusion of deformation and orientation effects of the decaying products change the fragment potential energy surface (PES) quite significantly and hence it creates remarkable contribution in deciding the decay process.

As a consequence, the relative preformation probabilities P_0 for all the fragments change in the ground state decay of parent nucleus. Similarly, the scattering potential (barrier position as well as height) is also modified with deformation and orientation effects of outgoing fragments included, thereby affecting the tunneling through barrier, and hence the penetrability P. Here the nuclei are considered to have the "optimum" orientations for the cold ground state decay process, i.e., the deformed cluster and daughter nuclei are in an elongated, non-compact configuration denoted θ_i^{opt}.

Although generalized orientations seem to play significant contribution in deciding the decay path of a radioactive parent. But in present calculations we have confined ourselves to optimum orientations only. Table 3.1 shows the comparison between the experimental and calculated cluster decay half lives of various parent nuclei using Preformed Cluster Model (PCM) of Gupta et al., by taking the binding energies from Moller- Nix (1995). Table 3.1 shows the respective cluster decays of various parent nuclei, i.e. $^{228, 230}$Th, ^{232,234,238}U, ^{236,238}Pu, ^{242}Cm.

It is relevant to mention here that the octupole and hexadecapole deformations might prove useful but it has been experienced that the extrapolated β_4 (hexadecapole) deformations are needed to be handled with case at least in the domain of light mass clusters. In light of this, we have confined our calculations to quadrupole deformations only. We have calculated the decay half lives of 14 clusters emitted from even-even parents of Th, U, Pu and Cm isotopes. It is clear from Table 3.1 that our PCM calculated half life values find nice comparison with the available experimental data except for the emission of ^{25}Ne cluster from ^{234}U. This is the case of an odd cluster emission and the contribution of β_4 values might be useful in the said case. In other words inclusion of β_3, β_4 contributions may improve the comparison for ^{25}Ne cluster emission from ^{234}U parent nucleus.

It is important to mention here that the only fitted parameter of the model i.e. ΔR is varied between (-0.5 to +0.5 fm) in order to fit the experimental data. The choice of +ve ΔR means that the entry level for penetration is shifted toward the barrier height position and –ve ΔR means that the entry point for penetration is shifted away from the barrier height position. Though all the studied clusters do find a significant contribution from the deformation and orientation effects i.e. the use of deformations (β_2 only in this case) and optimum orientations seem to influence the decay process of all the clusters studied. However, we intend to discuss the exclusive role played by these deformations and orientations in case of heaviest cluster formed in the decay of ^{242}Cm.

In the decay of ^{242}Cm we observe that the PCM calculations can fit the observed decay half life for the β_2 deformations with optimum orientations at ΔR values equal to (ΔR = -0.3 fm).

TABLE 3.1: Half-life times and other characteristic quantities for cluster decay of various parent nuclei. The calculations are made by using Preformed Cluster-decay Model (PCM) of Gupta and collaborators, for case of β_2 alone. The impinging frequency is u_0 ~10^{21} s^{-1} for each case. $Q_{M.N.}$ refers to Q-value calculated by using the binding energies of Moller et al [Ref. 40 of Chapter 2].

				Half-lives $(\log_{10} T_{1/2})s$ PCM	
Decay	N/Z	R_a	$Q_{M.N.}$	β_2	Expt.
$^{228}Th \rightarrow ^{20}O + ^{208}Pb$	1.53	R_t + 0.5	45.91	20.40	20.87
$^{230}Th \rightarrow ^{24}Ne + ^{206}Hg$	1.55	R_t + 0.5	58.57	24.19	24.64
$^{232}U \rightarrow ^{24}Ne + ^{208}Pb$	1.52	R_t + 0.25	62.03	21.58	21.05
$^{232}U \rightarrow ^{28}Mg + ^{204}Hg$	1.52	R_t - 0.3	74.06	23.28	>22.65
$^{234}U \rightarrow ^{24}Ne + ^{210}Pb$	1.54	R_t + 0.5	59.30	25.99	25.06
$^{234}U \rightarrow ^{25}Ne + ^{209}Pb$	1.54	R_t + 0.5	56.67	30.33	25.06
$^{234}U \rightarrow ^{26}Ne + ^{208}Pb$	1.54	R_t + 0.5	58.65	26.49	25.06
$^{234}U \rightarrow ^{28}Mg + ^{206}Hg$	1.54	R_t - 0.4	74.22	25.53	25.54
$^{236}Pu \rightarrow ^{28}Mg + ^{208}Pb$	1.51	R_t - 0.5	78.75	20.33	21.67
$^{238}U \rightarrow ^{34}Si + ^{204}Pt$	1.58	R_t +0.215	85.82	29.03	29.04
$^{238}Pu \rightarrow ^{28}Mg + ^{210}Pb$	1.53	R_t - 0.4	75.83	25.63	25.70
$^{238}Pu \rightarrow ^{30}Mg + ^{208}Pb$	1.53	R_t	76.82	25.29	25.70
$^{238}Pu \rightarrow ^{32}Si + ^{206}Hg$	1.53	R_t + 0.5	90.03	25.16	25.28
$^{242}Cm \rightarrow ^{34}Si + ^{208}Pb$	1.52	R_t - 0.3	95.78	23.49	23.24

The comparison graphs are plotted for fragmentation potential (V), preformation probability (P_0) and penetration probability (P) for the decay $^{242}Cm \rightarrow ^{34}Si + ^{208}Pb$ at $R_a = R_t + \Delta R$ (ΔR = -0.3 fm) at ℓ=0 for the case of spherical as well as quadrupole deformation β_2. It is relevant to mention here that in case of spherical choice this ΔR values changes from – 0.3 fm to 0 fm in order to fit the experimental data which is a

clear signature that deformations and orientations do play a significant role in deciding the decay process of a nuclear system.

Another quantity of interest for the calculations of decay constant (λ) or half life time ($T_{1/2}$) is the preformation factor P_0. The behavior of preformation probability P_0 explicitly depends on the fragmentation potential V (A_2). The fragmentation potential for ^{242}Cm is depicted in figure 3.1.

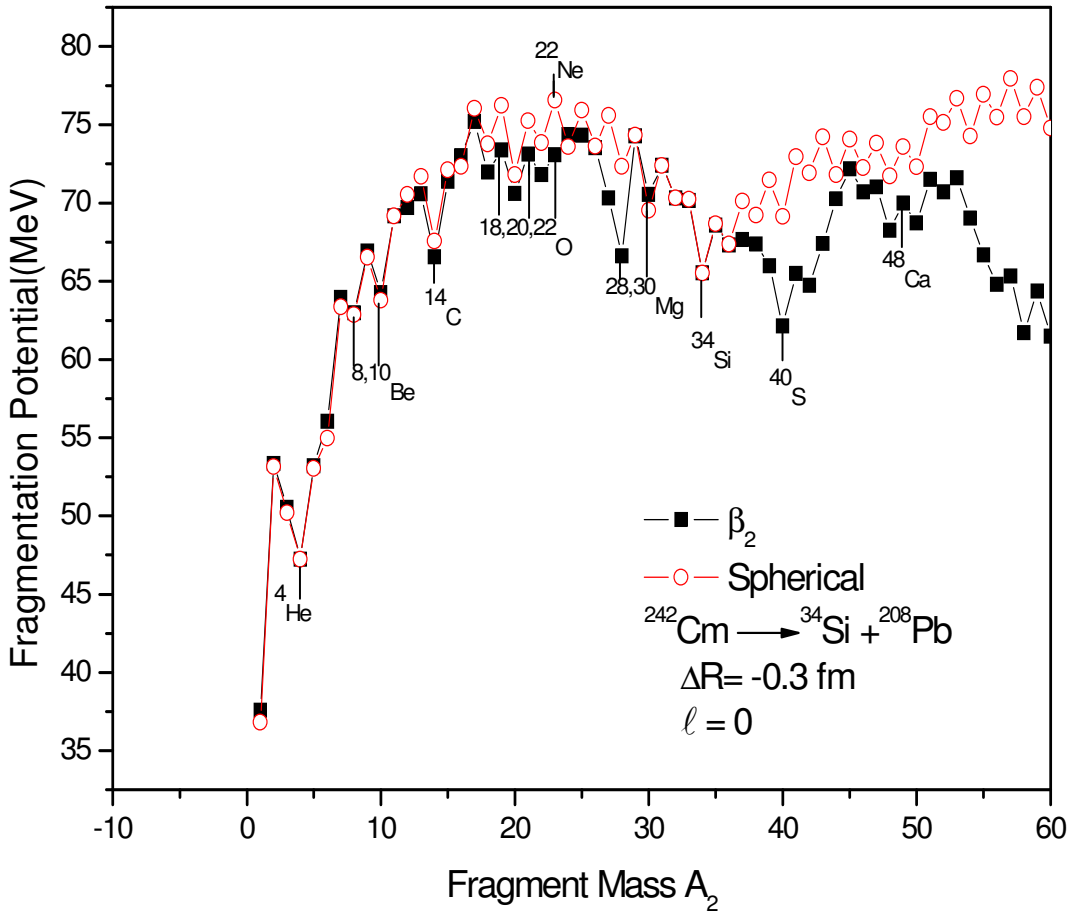

Figure 3.1: Fragmentation potential for the decay of 242Cm→^{34}Si + ^{208}Pb at ℓ = 0 at $R_a = R_t + \Delta R$ (ΔR = -0.3 fm) for the case of spherical compared with quadrupole deformation β_2 alone.

Here we have plotted the cases of spherical vs. quadrupole deformations β_2 alone for all the possible fragmentations of the parent nucleus. We notice that the inclusion of deformations and orientations of nuclei in V (A_2) play a silent role for the lighter clusters up to A_2 (mass of cluster) = 15. On the other hand, inclusion of deformations and orientations effects change the potential energy surface (PES) significantly for heavier clusters with $A_2 > 15$.

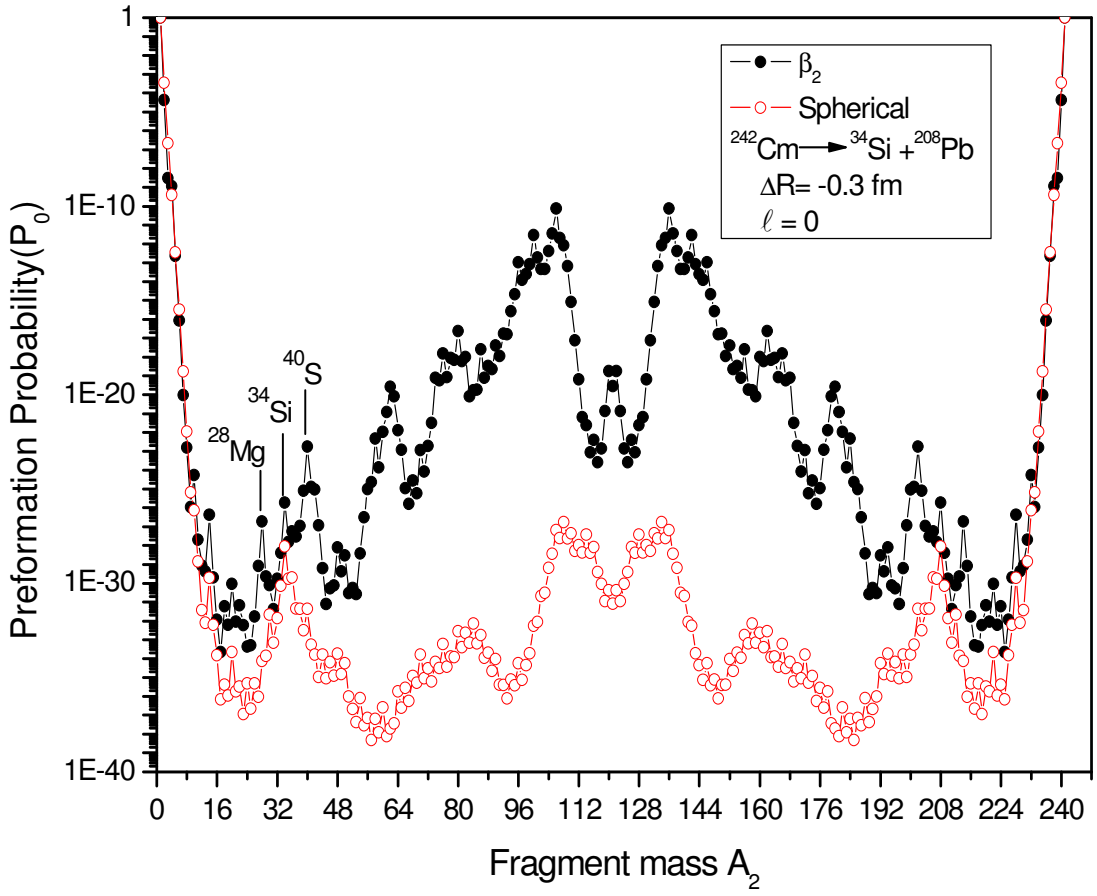

.

Figure 3.2: Preformation probability P_0 as a function of fragment mass A_2 for the decay of ^{242}Cm→^{34}Si + ^{208}Pb at $R_a = R_t + \Delta R$ (ΔR = -0.3 fm) at ℓ =0 for the case of deformed β_2 as well as spherical choice.

It is important to note that α nucleus structure remains intact for spherical as well as deformed considerations. The ^{34}Si cluster shows the expected minima in fragmentation plot for spherical as well as the deformed case. Beside this, the clusters ^{28}Mg and ^{40}S also show preferential cluster formation. The ^{28}Mg possibility is ruled out via penetration probability calculations whereas the origin and cause of ^{40}S cluster needs further investigations before reaching at an explicit conclusion.

In figure 3.2 we observe that there is no significant change in PES for the cluster mass up to A_2~15. However, for A_2 > 15 many pronounced peaks are observed in going from spherical to deformed (β_2 alone). For example in figure.3.2, the ^{28}Mg, ^{34}Si and ^{40}S clusters show enhanced peaks for the deformed choice of fragmentation. It is worth noticing here that one gets relatively pronounced structure with deformed fragmentation as compared to spherical case. However the overall distribution remains similar i.e. we find symmetric/near symmetric fragmentation for both the choices.

It is well established fact that due to deformations, the barrier height gets reduced and barrier position gets elongated, thereby affecting the tunneling penetrability P. Note that the calculated decay constant λ (or half- life $T_{1/2}$) depend on barrier Penetration probability P, and hence on inclusion/ or non- inclusion of deformations and orientations of nuclei. Therefore the role of deformations and orientations seems important in order to access the emission path of a cluster from parent nucleus. In order to estimate such effects we have calculated penetration probability (P) as a function of fragment mass (A_2). The Penetration probability as a function of fragment mass is shown in fig.3.3 for the decay of ^{242}Cm→^{34}Si + ^{208}Pb at ℓ =0 for the spherical as well as deformed choice of fragmentation process.

From figure 3.2 also it is clearly evident that deformations and orientations play a significant role in the clusterization process. It is worth notification that the ^{34}Si cluster shows an enhanced penetrability justifying the cluster formation in the decay of ^{242}Cm. Clearly the prominence of ^{24}Mg is ruled out because of lower P value however emergence of ^{40}S needs further study, possibly the inclusion of generalized orientations and the inclusion of higher multipole deformations may resolve the issue.

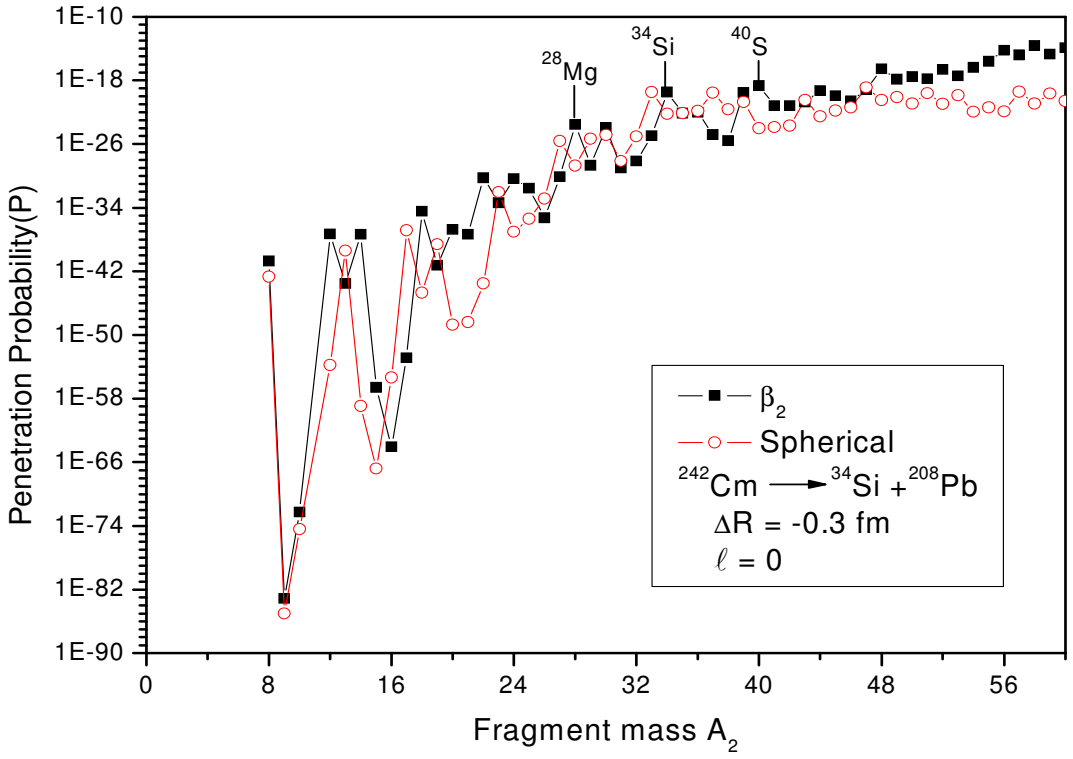

Figure 3.3: Penetration probability (P) as a function of fragment mass A_2 for the decay of $^{242}Cm \rightarrow ^{34}Si + ^{208}Pb$ at $R_a = R_t + \Delta R$ (ΔR = -0.3 fm) at ℓ =0 for the case of deformed β_2 as well as spherical choice.

One may conclude that the preformation probability P_0 as well as penetrability P gets influenced by the inclusion of deformation/orientations which further effects the decay constant and half life time values accordingly. In other words the decay constant and half life times get greatly influenced by the inclusion of deformation and orientation effects. So one may conclude that proper understanding of nuclear shapes and along with the relative orientations of target/projectile is essential to make concrete and explicit predictions/verifications of the clusterization process.

Chapter 4

SUMMARY

Summary

Cluster radioactivity is a process in which we study the emission of clusters heavier than α particle and smaller than fission fragments. It is a well established fact that this ground state decay depends heavily on the shell closure effects of nuclear systems in heavy mass region. Beside this, Q-value of the reaction seems to play crucial role in deciding the clusterization/fragmentation process in this rare nuclear phenomena.

In recent times our understanding has grown regarding the formation and decay process of nuclear systems, and a lot many exotic experiments and advanced theoretical developments have enabled us to study the nuclear behavior in new perspective. In view of these developments it has been established that the deformation and orientations of entrance and exit channel fragments influence the nuclear dynamics immensely. In view to these developments it seems relevant and important to investigate the role of deformations and orientations in the relatively rare decay process known as cluster radioactivity.

Keeping this in mind the role of deformations and orientations of nuclei is studied in the cluster radioactivity process. Our calculations using PCM of Gupta and collaborators clearly depict that the deformations and orientations have significant effects on the calculated decay half-lives. The measured data on cluster decay half-lives is tested for the clusterization of even-even isotopes of Th, U, Pu and Cm using the Preformed Cluster Model (PCM) where the effects of deformations are included up to quadrupole deformation (β_2) only and the criteria of optimum orientations is used.

The interesting point is that both the preformaton factor P_0 and penetrability P are shown to get modified with the inclusion of deformation and orientation effects. Moreover, unlike P, the P_0 is effected not only due to the shapes of parent, daughter and cluster nuclei, but also due to the shapes of all other possible fragmentations of the decaying parent nucleus and therefore it becomes extremely desirable to include the

deformation/orientation effects in the clusterization process. Our calculated half lives for the isotopes of Th, U, Pu and Cm find an excellent comparison with the available experimental data except for the ^{25}Ne decay from ^{234}U. It seems the inclusion of higher multipoles along with generalized orientation consideration may resolve the issue. The existence of ^{34}Si is explicitly established via PCM calculations in the decay of ^{242}Cm. The comparative emergence of other clusters like ^{28}Mg and ^{40}S is also addressed.

The present study clearly points out the importance of deformation and orientation effects in cluster decays of radioactive nuclei. We have confined our self to the β_2 deformation only. However, the inclusions of higher multiple deformations is desirable but, their contribution needs a closer look before reaching at any discrete conclusion since the (calculated) data used so far for β_3 and β_4 may not be adequate because of extrapolation criteria adopted to generate this database. It seems that proper inclusion of higher multipole deformations along with generalized orientation contributions may prove important in deciding the cluster decay paths of various clusters. This study is of great importance in order to establish the clusterization process of fragments higher than α particle and smaller than fission fragments.